https://doi.org/10.5194/acp-2020-1187
Preprint. Discussion started: 25 November 2020

Atmospheric Chemistry and Physics Discussions

Chemical characterization of oxygenated organic compounds in gas-phase and particle-phase using iodide-CIMS with FIGAERO in urban air

Chenshuo Ye[1], Bin Yuan[2,3,*], Yi Lin[2,3], Zelong Wang[2,3], Weiwei Hu[4], Tiange Li[2,3], Wei Chen[4], Caihong Wu[2,3], Chaomin Wang[2,3], Shan Huang[2,3], Jipeng Qi[2,3], Baolin Wang[5], Chen Wang[5], Wei Song[4], Xinming Wang[4], E Zheng[2,3], Jordan E. Krechmer[6], Penglin Ye[7], Zhanyi Zhang[2,3], Xuemei Wang[2,3], Douglas R. Worsnop[6], Min Shao[2,3,1,*]

[1] College of Environmental Sciences and Engineering, Peking University, Beijing 100871, China

[2] Institute for Environmental and Climate Research, Jinan University, Guangzhou 511443, China

[3] Guangdong-Hongkong-Macau Joint Laboratory of Collaborative Innovation for Environmental Quality, Guangzhou 511443, China

[4] Guangzhou Institute of Geochemistry, Chinese Academy of Sciences, Guangzhou 511443, China

[5] School of Environmental Science and Engineering, Qilu University of Technology, Jinan 250353, China

[6] Aerodyne Research, Inc. 45 Manning Rd., Billerica, MA, USA

[7] Shanghai Key Laboratory of Atmospheric Particle Pollution and Prevention (LAP[3]), Department of Environmental Science and Engineering, Fudan University, Shanghai 200438, China

*Correspondence to: byuan@jnu.edu.cn; mshao@pku.edu.cn

https://doi.org/10.5194/acp-2020-1187
Preprint. Discussion started: 25 November 2020

Atmospheric Chemistry and Physics Discussions

Abstract

The characterization of oxygenated organic compounds in urban areas remains a pivotal gap in our understanding of the evolution of organic carbon under polluted environments, as the atmospheric processes involving interactions between organics and inorganics, anthropogenic pollutants and natural emissions lead to formation of various and complex secondary products. Here, we describe measurements of an iodide chemical ionization time-of-flight mass spectrometer installed with a Filter Inlet for Gases and AEROsols (FIGAERO-I-CIMS) in both gas-phase and particle-phase at an urban site in Guangzhou, a typical mega-city in southern China, during the autumn of 2018. Abundant oxygenated organic compounds containing 2~5 oxygen atoms were observed, including organic acids, multi-functional organics typically emitted form biomass burning, oxidation products of biogenic hydrocarbons and aromatics. Photochemistry played dominant roles in the formation of gaseous organic acids and isoprene-derived organic nitrates, while nighttime chemistry contributed significantly to the formation monoterpene-derived organic nitrates and inorganics. Nitrogen-containing organic compounds occupied a significant fraction of the total signal in both gas and particle phases, with elevated fractions at higher molecular weights. Measurements of organic compounds in particle phase by FIGAERO-I-CIMS explained 24% of the total organic aerosol mass measured by aerosol mass spectrometer (AMS), and the fraction increased for more aged organic aerosol. The systematically interpretation of mass spectra of the FIGAERO-I-CIMS in urban of Guangzhou provides a holistic view of numerous oxygenated organic compounds in the urban atmosphere, which can serve as a reference for the future field measurements by FIGAERO-I-CIMS in polluted urban regions.

https://doi.org/10.5194/acp-2020-1187
Preprint. Discussion started: 25 November 2020

Atmospheric Chemistry and Physics Discussions

1 Introduction

In urban air, atmospheric chemical processes are varied and complex, as the result of large emissions of both anthropogenic pollutants and biogenic volatile organic compounds, associated with strong interactions with each other (He et al., 2014; Karl et al., 2018; Shrivastava et al., 2019). Consequently, strong formation of secondary pollutants, e.g. ozone and secondary organic aerosol (SOA), are observed in urban and downwind regions (Huang et al., 2015; Zhang et al., 2014). Previous literature suggests that oxygenated organic compounds provide a vital link between advanced chemical mechanisms and the model-observation discrepancy for many unaddressed issues in atmospheric chemistry. They are supposed to be the top candidates for missing OH reactivity observed in various environments including pristine rainforests and urbanized areas (Noelscher et al., 2016; Yang et al., 2016, 2017). The photolysis of carbonyls serves as a critical radical source driving ozone formation in highly polluted industrialized areas (Edwards et al., 2014; Liu et al., 2012; Xue et al., 2016). Although it has been discovered a long time ago that oxygenated organic compounds make up a substantial fraction of submicron aerosol mass (Kroll and Seinfeld, 2008), enormous difficulty still exists in accurately predicting formation and evolution of SOA (de Gouw et al., 2005; Hodzic et al., 2010; Volkamer et al., 2006).

One of the biggest problems hindering our understanding in the role of oxygenated organic compounds is the characterization of these extremely complicated and diverse chemicals which encompass tens of thousands of individual species spanning a wide range of volatility. Chemical ionization mass spectrometry (CIMS) is a powerful technique for the molecular-level characterization of oxygenated organic compounds because of the following advantages (Zhao, 2018): direct measurements and fast time response to capture the rapid temporal change of short-lifetime intermediates; soft ionization providing chemical information on molecular level; selective ionization ensuring measurements for specific classes of species. Iodide anion ionizes species mainly through adduction (Iyer et al., 2016) and is used for the detection of oxygenated organic compounds particularly organics with 2~5 oxygen atoms (Lee et

https://doi.org/10.5194/acp-2020-1187
Preprint. Discussion started: 25 November 2020


Atmospheric Chemistry and Physics Discussions

al., 2014; Lopez-Hilfiker et al., 2016; Riva et al., 2019). It has been shown that I-CIMS is an excellent technique to investigate oxidation processes of volatile organic compounds (VOCs) and formation of SOA (Isaacman-VanWertz et al., 2018). Installed with a thermal desorption inlet that collects and heats aerosol to evaporate organic coatings, e.g. Filter Inlet for Gases and AEROsols (FIGAERO, Lopez-Hilfiker et al., 2014), the CIMS instruments are capable of analyzing particle-phase species and gas-particle partitioning in a semi-continuous way (Stark et al., 2017; Stolzenburg et al., 2018).

Although there is a growing trend for applications of FIGAERO-I-CIMS in field campaigns, most work has been mostly performed in forest or rural areas (Huang et al., 2019; Hunter et al., 2017; Lee et al., 2016, 2018b), and systematic analysis of measurements in urban atmosphere by FIGAERO-I-CIMS is still limited (Le Breton et al., 2018b). In this study, we present measurement results using this instrumentation during a coordinated campaign in Guangzhou, a megacity in the Pearl River Region of China. We provide an overview of gas-phase and particle-phase oxygenated species detected in the mass spectra of FIGAERO-I-CIMS during the campaign. The bulk chemical properties of organic compounds in both gas phase and particle phase will also be discussed.

2 Methods

2.1 Measurement site and supporting data

Measurements were conducted during the coordinated campaign "Particles, Radicals and Intermediates from oxiDation of primary Emissions over the Great Bay Area" (PRIDE-GBA) in October and November 2018. The Great Bay Area (GBA) refers to a highly industrialized and urbanized area in southern China, including two Special Administrative Regions of Hong Kong and Macao, and nine cities surrounding the Pearl River estuary. Affected by the subtropical monsoon climate, the weather in the region was characterized by high temperatures and relative humidity (RH) as well as sufficient sunshine (Wang and LinHo, 2002; Yihui and Chan, 2005). The city of Guangzhou lies on the north of the GBA and south to the mountains. Therefore, the city

https://doi.org/10.5194/acp-2020-1187
Preprint. Discussion started: 25 November 2020


Atmospheric Chemistry and Physics Discussions

is extensively influenced by both anthropogenic and biogenic emissions. The urban site in Guangzhou was located at Guangzhou Institute of Geochemistry, Chinese Academy of Sciences (23.14°N, 113.36°E). Online instruments sampled from inlets set up in laboratories on the eighth-floor or ninth-floor (about 25 meters above the ground).

In addition to FIGAERO-I-CIMS discussed later, measurements data from a suite of other instruments were also used in this work. A high-resolution time-of-flight aerosol mass spectrometer (HR-ToF-AMS, Aerodyne Research, Inc.) was deployed to provide chemical composition and many other parameters of ambient aerosol including f60, liquid water content (LWC), particulate organic nitrates and elemental ratios (Hu et al., 2016, 2018). The parameter f60 is the ratio of the integrated signal at m/z 60 to the total signal of organic components and is used as a tracer for biomass burning emissions (Cubison et al., 2011). LWC of aerosol was taken as the sum of water contributed by inorganic components which was predicted by ISORROPIA II model and organic components (Fountoukis and Nenes, 2007; Guo et al., 2015). Organic nitrates were separated from NH_4NO_3 based on their difference in NO_2^+/NO^+ ratio (Fry et al., 2013). The calculation method of elemental ratios based on AMS data has been described elsewhere (Aiken et al., 2007; Canagaratna et al., 2015). Detailed information about AMS measurements from the PRIDE-GBA campaign are forthcoming in a separate manuscript. An online GC-MS/FID (Wuhan Tianhong Instrument Co., Ltd) and a proton transfer reaction time-of-flight mass spectrometer (PTR-ToF-MS, Ionicon Analytic GmbH) (Yuan et al., 2017) served as the analytical techniques for measuring isoprene and other VOCs (e.g. monoterpenes, aromatics and a few oxygenated VOCs) (Wu et al., 2020), respectively. Trace gases (CO, O_3, NO and NO_2) were measured by commercial gas monitors (Thermo Fisher Scientific Inc.) (Wang et al., 2020c). Photolysis rates were measured by PFS-100 photolysis spectrometer (Focused Photonics Inc.). Fig. S1 shows the diel changes of trace gases, $j(NO_2)$ and important VOCs (isoprene, monoterpenes, toluene and benzene). Temperature and RH were measured by a Vantage Pro2 weather station (Davis Instruments Corp.). Temperature during campaign was between 17 and 33°C with an average of 24°C and RH was

https://doi.org/10.5194/acp-2020-1187
Preprint. Discussion started: 25 November 2020


Atmospheric Chemistry and Physics Discussions

between 27 and 97% with an average of 70%.

2.2 FIGAERO-I-CIMS

2.2.1 Experimental setup

Our instrument consists of a Filter Inlet for Gases and AEROsols (FIGAERO) and a time-of-flight chemical ionization mass spectrometer coupled with iodide ionization source (Bertram et al., 2011; Lee et al., 2014; Lopez-Hilfiker et al., 2014). The FIGAERO is a multi-port inlet assembly following a two-step procedure alternating between gas mode in which online measurements of gases and semi-continuous sampling of particle-phase species are conducted, and particle mode in which particulate composition is investigated via thermally desorption (Lopez-Hilfiker et al., 2014; Thornton et al., 2020). Iodide reagent ions provide a very "soft" ionization technique with little ionization-induced fragmentation and selective detection towards multi-functional organic compounds, making it suitable for chemical speciation of thousands of complicated oxygenated compounds in the atmosphere (Hyttinen et al., 2018; Iyer et al., 2016; Lee et al., 2014; Riva et al., 2019).

The sample air was drawn into the ion molecule reaction (IMR) chamber where it intersected and reacted with iodide ions generated by flowing 2 mL/min 1000 ppm methyl iodide in 2.4 L/min N_2 through an X-ray source. The pressure in the IMR chamber was maintained at 370~390 mbar. Equipped with a long time-of-flight mass analyzer, our instrument was configured to measure singularly charged ions up to 603 Th with a mass resolving power of 10000~11000 m/Δm during the campaign (see Fig. S2).

Ambient air was continuously sampled through two inlets sticking outside the window on ninth-floor of a building. One was a 3-meter PFA tubing (1/4-inch OD) for gas phase sampling, through which roughly 9 L/min air was drawn, and 2 L/min was taken into the instrument for gas measurements. The residence time was 0.35 seconds. The gas sampling line inside the room was covered by heat insulation associated with a heating cable to minimize condensation on the tubing surface. Another one was a 3.8-meter metal tubing (3/8-inch OD) for particle phase fitted with a $PM_{2.5}$ cyclone and a

https://doi.org/10.5194/acp-2020-1187
Preprint. Discussion started: 25 November 2020

Atmospheric Chemistry and Physics Discussions

Nafion dryer (Perma Pure, model PD-07018T-12MSS) to reduce water content in the sampled air. The particle phase inlet was drawn by about 10 L/min, 3.8 L/min of which was collected on PTFE membrane filters (Zefluor®, Pall Inc., USA).

The FIGAERO worked in a cyclical 1-hour pattern with two modes: measuring gas for the first 24 minutes while simultaneously collecting particles on the filter; and then analyzing the particle-phase collection for another 36 minutes. Fig. S3 displays the two sampling setups of the FIGAERO. In every 24-minute gas mode, ambient air was measured for the first 21 minutes, followed by 3-minute gas background by over flushing zero air at 5 L/min through a pinhole just in the front of the IMR. In the remaining 36 minutes, the components of collected particles were thermally desorbed and introduced into the CIMS with 2 L/min N_2 carrier gas. Schematic diagram of working modes and temperature profile of FIGAERO heating in a single cycle is shown in Fig. S4. Particle background was determined every 6^{th} 1-hour running cycles, during which the particles passed through a filter (Parker Balston, model 9922-11-CQ) before being collected on the PTFE membrane filter.

2.2.2 Calibration experiments

Using various techniques, we calibrated dozens of chemical compounds in the laboratory. Table S1 summarizes the calibrated species and corresponding calibration methods. (1) Gas cylinders are commercially available for a few species (e.g. chlorine, hydrogen cyanide). The gaseous standards were diluted down to different concentrations and then introduced to the CIMS. (2) For those VOCs of which standards are liquid or solid, solutions with known concentrations are made and then vaporized using the liquid calibration unit (LCU, Ionicon Analytic GmbH) to provide gaseous standards. (3) Commercial permeation tubes are available for some species (e.g. nitric acid). (4) Some gaseous chemicals were generated in the laboratory. For example, isocyanic acid was generated from thermal decomposition of cyanuric acid in a diffusion cell (Wang et al., 2020c), and dinitrogen pentoxide was generated via the reaction of ozone with excess nitrogen dioxide in a flow reactor (Bertram et al., 2009). (5) Compounds of low vapor pressure were calibrated through the FIGAERO (Lopez-

https://doi.org/10.5194/acp-2020-1187
Preprint. Discussion started: 25 November 2020


Atmospheric Chemistry and Physics Discussions

Hilfiker et al., 2014). Briefly, certain amounts of target species dissolved in organic solvents (e.g. isopropanol or acetone) were injected onto the PTFE filter of the FIGAERO using a syringe, and the droplet was then subjected to a temperature-programmed thermal desorption by N_2 gas. The sensitivity for particle phase was determined as the peak areas under thermogram profiles versus the amount of injected calibrant.

In addition to sensitivity calibration, the effect of humidity on the sensitivity for various species was also investigated in the laboratory. The humidity-dependence curves for some of the calibrated species are shown in Fig. S5. Low-molecular-weight acids, e.g., formic acid and nitric acid, tend to be more sensitive to the humidity changes than multi-functional compounds. Similar tendency of multi-functional compounds associated with less humidity dependence was also reported in previous work (Lee et al., 2014).

In the later part of the campaign (after Oct. 22), an isotopically labeled formic acid (DCOOH, Cambridge Isotope Laboratories, Inc.) permeation tube held at constant temperature (65 ℃), was mixed with 10 mL/min N_2 and continuously delivered into the entrance of sampling inlet in order to derive a humidity dependence function from field measurements. Fig. S5 presents that DCOOH signals during the campaign exhibited consistent dependence curve with formic acid obtained in the laboratory. We applied humidity correction to the species with humidity-dependent curve determined in the laboratory, including C1-C5 organic acids, catechol, HNCO, Cl_2 and HNO_3. For other compounds, humidity correction was not applied, as there is no universal pattern of humidity dependence for all detected species and multi-functional compounds that comprise the majority of species measured by FIGAERO-I-CIMS are usually less influenced by humidity.

The measured concentration of DCOOH was steady after applying humidity correction (Fig. S6g), indicating the stability of our instrument. In addition, we also performed field calibrations throughout the campaign to check the instrument status by spotting a solution mixture of levoglucosan, heptaethylene glycol and octaethylene glycol on the FIGAERO filter every 2 ~ 3 days (Fig. S6). Multiple-point calibrations

https://doi.org/10.5194/acp-2020-1187
Preprint. Discussion started: 25 November 2020


Atmospheric Chemistry and Physics Discussions

for these organic species were performed in the beginning and the end of the campaign. The concentration of the solution used in the first two calibration experiments was too high, so we prepared a new solution for calibrations after November. The relative changes of the determined calibration factors in November were within 50% for the calibrated species.

2.2.3 Data processing

The TofWare software (version 3.0.3; Tofwerk AG, Switzerland) was used to conduct the high-resolution peak fitting for the mass spectra data of ToF-CIMS, including mass calibration, instrumental parameters optimization (peak shape and peak width) and bunch fitting of high-resolution peaks (Stark et al., 2015). In this study, the signals of ions were normalized to the sum signals of I^- and H_2OI^- at 10^6 cps. Hourly particle-phase data were obtained by integrating the sum signals of each ion during each FIGAERO desorption period, i.e., peak areas. Background corrected signals were obtained by subtracting linearly interpolated background signals from ambient signals (and peak areas) for ions in the gas (and particle) phase.

In order to determine the sensitivities of uncalibrated species, voltage scanning procedure was performed from time to time throughout the campaign covering different times of the day (Iyer et al., 2016; Lopez-Hilfiker et al., 2016). Here, we selected four representative periods including morning, afternoon, evening and night on polluted days. By performing sigmoidal fitting on the remaining signals as a function of voltages, a dV_{50} value of each ion from each period was determined at which voltage half of one kind of ion dissociated (Lopez-Hilfiker et al., 2016). We observed a positive correlation between the sensitivities of the ions relative to maximum sensitivity and their average dV_{50} values (Fig. S7), consistent with previous studies (Isaacman-VanWertz et al., 2018; Lopez-Hilfiker et al., 2016). This relationship was used to calculate response factors for uncalibrated species, after taking into account relative transmission efficiency for the ions (see Section S1 in the Supplement for detailed analysis).

3 Results and discussion

3.1 Overview of detected species in the mass spectra

https://doi.org/10.5194/acp-2020-1187
Preprint. Discussion started: 25 November 2020

Atmospheric Chemistry and Physics Discussions

We identify1334 ions adducted with iodide from the mass spectra, among which 427 are charged closed-shell organics containing only C, H, O elements ($C_xH_yO_zI^-$) and 388 are charged closed-shell organics containing C, H, O and N elements ($C_xH_yN_{1,2}O_zI^-$). For species with the formula of $C_xH_yO_z$, x ranges from 1 to 20; y is an even number and no more than 2x+2; z is greater than or equal to 2. The range of carbon number x for the ions with $C_xH_yN_{1,2}O_z$ is the same as the ions with $C_xH_yO_z$. For species containing one nitrogen ($C_xH_yNO_z$), y is an odd number and less than 2x+2; z is larger than or equal to 2. For species containing two nitrogen atoms ($C_xH_yN_2O_z$), y is an even number and less than 2x+1; z is larger than or equal to 4.

The campaign-averaged mass spectra of detected ions in both gas and particle phases are shown in Fig. 1. In general, molecules in particle-phase have larger molecular weights compared to gas-phase compounds. Signals in the mass range of 150 ~ 300 Th comprise a large fraction of gas-phase compounds, and concentrations in the gas phase decrease quickly with m/z higher than 250 Th. For comparison, the detected signals in the particle phase are mainly distributed within the range of 200 ~ 320 Th.

We compare the concentration for various ions between the daytime (10 am ~ 6 pm) and nighttime (10 pm ~ 6 am), by determining concentration ratios between at night and during the daytime (Fig. 2). Most species have higher concentrations during the daytime, especially for relatively volatile compounds in gas-phase, despite the fact that lower boundary layer height at night should increase nighttime mixing ratios, as behaved for many primary gases, e.g. CO (Fig. S1) (Wu et al., 2020). The higher concentrations during the daytime for most species detected by FIGAERO-I-CIMS suggest the dominant role of photochemical induced oxidation in forming these oxidized compounds. In addition to typical nocturnal species including nitryl chloride ($ClNO_2I^-$), chlorine nitrate ($ClONO_2I^-$) and dinitrogen pentoxide ($N_2O_5I^-$), higher concentrations for the ions of $C_6H_{10}O_5I^-$ and $C_6H_{12}O_5I^-$ were also observed, which will be discussed in next section. A large number of particulate N-containing organics increase during the night as well, as shown by mass defect diagrams of $C_xH_yO_z$ and $C_xH_yN_{1,2}O_z$ color coded by the night to day ratios (Fig. S8).

https://doi.org/10.5194/acp-2020-1187
Preprint. Discussion started: 25 November 2020


Atmospheric Chemistry and Physics Discussions

The ions in the mass spectra of FIGAERO-I-CIMS are classified and interpreted in the following Section 3.2-3.7, including monosaccharide-derived compounds (with brown tags in Fig. 1), oxygenated aromatics (with purple tags), organic acids (with pink tags), oxidation products of biogenic volatile organic compounds (BVOCs, with green tags), sulfur-containing compounds, and inorganics (with blue tags). After going through detailed analysis in the species level, Section 3.8 will provide an overall picture about bulk chemical characteristics of detected organic compounds in terms of the distributions of average carbon oxidation states, carbon number and oxygen number. Lastly, Section 3.9 will compare our measurement of organic aerosol (OA) with AMS data.

3.2 Monosaccharide-derived compounds

$C_6H_{10}O_5$ and $C_6H_{12}O_5$ are two of a few $C_xH_yO_z$ compounds with higher concentrations at night, and they are highly correlated with each other in aerosol (r=0.92). Previous work assigned them as monosaccharide derived compounds emitted from biomass burning (Bhattarai et al., 2019; Qi et al., 2019; Reyes-Villegas et al., 2018; Simoneit et al., 1999).

In this campaign, $C_6H_{10}O_5$ was detected mostly in the particle phase (F_p=0.83± 0.08) with an average concentration of 0.073±0.076 μg/m^3, and the diurnal profile started increasing during dusk, reaching a peak at about midnight and then fell off, as shown in Fig. 3. The mass fraction of $C_6H_{10}O_5$ in OA had a similar diurnal profile, and the ratios of $C_6H_{10}O_5$ to CO increased at night (from 1.5×10^{-4} to 4.1×10^{-4} μg·m^{-3}/ppb, Fig. 3c), both suggesting enhanced emissions of this compound related with combustion activities at night. Furthermore, particle-phase $C_6H_{10}O_5I^-$ closely resembled the m/z 60 fragment in AMS mass spectra (r=0.75), which is an identified tracer of biomass burning OA produced from the decomposition of levoglucosan and similar compounds during detection by AMS (Brege et al., 2018; Cubison et al., 2011; Schneider et al., 2006). Therefore, $C_6H_{10}O_5$ was probably levoglucosan and its isomers (mannosan and galactosan), and $C_6H_{12}O_5$ was a similar monosaccharide compound emitted from biomass burning.

https://doi.org/10.5194/acp-2020-1187
Preprint. Discussion started: 25 November 2020

Atmospheric Chemistry and Physics Discussions

3.3 Oxygenated aromatic compounds

Combustion activities emit a great deal of compounds besides saccharides that the I-CIMS instrument can detect including nitro-aromatics and guaiacol derivatives (Gaston et al., 2016; Kong et al., 2021). Nitro-benzenediols ($C_6H_5NO_4I^-$) as well as the highly correlated homologue methyl nitro-benzenediols ($C_7H_7NO_4I^-$) (r=0.88 in the particle phase), exhibited double peaks in their diurnal profiles (Fig. 4). Concentrations of $C_6H_5NO_4$ and $C_7H_7NO_4$ was enhanced in the evening, similar to levoglucosan ($C_6H_{10}O_5$). Another concentration peaks at noon were also observed for $C_6H_5NO_4$ and $C_7H_7NO_4$. The scatterplot of $C_6H_5NO_4$ as the function of $C_6H_{10}O_5$ exhibited two different slopes at night and during the daytime (Fig. 5). This evidence suggests that primary emissions and secondary formation were both important contributors to nitro-aromatics during the campaign. Guaiacol derivatives may have similar sources with nitro-aromatics, as implied by the resemblance of the scatterplots of these two chemical classes versus levoglucosan (cf., Fig. S9 and Fig. 5).

Nitrophenols ($C_6H_5NO_3I^-$), methyl nitrophenols ($C_7H_7NO_3I^-$) and dinitrophenols ($C_6H_4N_2O_5I^-$) were the most significant components of nitro-aromatics in the gas phase. Despite the fact that nitrated phenols could be formed by photochemical oxidation from their aromatic hydrocarbon precursors (Wang et al., 2020a; Yuan et al., 2016), none of them peaked in the daytime, consistent with photolysis as a dominant chemical loss for these compounds (Chen et al., 2011; Yuan et al., 2016). Nitrophenols and methyl nitrophenols peaked in the evening, suggesting either NO_3 oxidation or primary emissions was important sources. It is interesting to observe that the peak concentration for $C_6H_4N_2O_5$ was later than the nitrophenols, in agreement with dinitrophenols as the oxidation products from nitrophenols (Harrison et al., 2005).

Several ions identified as oxidation products of aromatics, including $C_7H_6O_4I^-$, $C_7H_8O_4I^-$ and $C_7H_8O_5I^-$ (Mehra et al., 2020; Schwantes et al., 2017), were detected during the campaign. $C_7H_6O_4$ and $C_7H_8O_4$ correlated well with each other (r=0.72). High concentrations of $C_7H_6O_4$ and $C_7H_8O_4$ were mainly observed during the periods

https://doi.org/10.5194/acp-2020-1187
Preprint. Discussion started: 25 November 2020


Atmospheric Chemistry and Physics Discussions

with lower NO_X concentration, which is contrast to the variations of nitrophenols (Fig. S9). We observe the concentration ratios of $C_7H_8O_4I^-$ and $C_7H_7NO_3I^-$ were lower for higher NO_X concentrations (Fig. 5), consistent with the literature that formation of $C_7H_6O_4$ and $C_7H_8O_4$ is suppressed at high NO_X concentrations (Schwantes et al., 2017). $C_7H_8O_5$ was reported as the ring-retaining oxidation product of $C_7H_8O_4$ which is a typical oxidation product of toluene and cresol (Schwantes et al., 2017; Wang et al., 2020b), as well as the ring-scission products of aromatic hydrocarbons with more carbon atoms, e.g. trimethyl benzenes (Mehra et al., 2020). Given that $C_7H_8O_5$ closely followed with $C_7H_8O_4$ (r=0.93 in particles), toluene oxidation was probably the main contributor to this ion.

3.4 Organic acids

Organic acids were one of the most abundant species classes detected by I-CIMS (Fig. 1). Low-molecular-weight organic acids (e.g., formic, acetic, glycolic and pyruvic acid) constituted a significant fraction of signals in the mass spectra detected from gas phase. As shown in Fig. 6 (and also Fig. S10), they had very similar temporal trends with diel maxima in the afternoon, indicating photochemical oxidation played a dominant role in their formation (de Gouw et al., 2018; Yuan et al., 2015).

In contrast to monocarboxylic acids, dicarboxylic acids partitioned mostly to particle-phase. As the dominant dicarboxylic acids in aerosol (Kawamura and Bikkina, 2016; Mellouki et al., 2015), 94±5% and 74±13% (mean±standard deviation of F_p) of $C_2H_2O_4$ and $C_3H_4O_4$, assigned as oxalic and malonic acid, were found in particle-phase, respectively. The concentrations of $C_4H_6O_4$ are significantly lower compared to that of C2 and C3 homologous series, but $C_5H_8O_4$ and $C_6H_{10}O_4$ had unexpected higher abundances (Fig. 7). $C_5H_8O_4$ and $C_6H_{10}O_4$ had considerable fractions in the gas phase (45±13% and 43±11%), significantly higher than their C2 ~ C3 homologous series. These two compounds were correlated well with each other in temporal variations (r=0.97 and 0.91 in the gas and particle phases, respectively), and their diurnal variations were different from those of oxalic and malonic acid (Fig. 6). Therefore, dicarboxylic acids may not be the dominant contributing species for the two ions.

https://doi.org/10.5194/acp-2020-1187
Preprint. Discussion started: 25 November 2020


Atmospheric Chemistry and Physics Discussions

$C_5H_8O_4$ and $C_6H_{10}O_4$ have been observed from previous study on isoprene oxidation (Berndt et al., 2018, 2019), attributing them as epoxy hydroperoxyl carbonyl and accretion product, respectively. However, the relative contributions from these possibilities remain unclear.

In addition to the series of $C_nH_{2n-2}O_4$ (i.e. $C_2H_2O_4$, $C_3H_4O_4$), we also observed comparable concentrations of $C_nH_{2n-4}O_4$ ions, especially for carbon number of 4 and 5 ($C_4H_4O_4$ and $C_5H_6O_4$). Considering the double bonds in the molecules, $C_nH_{2n-4}O_4$ should be more reactive than $C_nH_{2n-2}O_4$, suggesting there were large sources for these compounds. Previous studies have reported photo-oxidation of aromatics can generate $C_nH_{2n-4}O_4$, including $C_4H_4O_4$ and $C_5H_6O_4$ (Brege et al., 2018; Kawamura et al., 1996; Kawamura and Bikkina, 2016). Our measurements during the campaign indicate that temporal trends of $C_4H_4O_4$ and $C_5H_6O_4$ followed well with those of aromatic hydrocarbons (Fig. S10b). As a result, we attributed $C_nH_{2n-4}O_4$ ions as oxidation products of aromatics in the urban air.

3.5 Oxidation products of Biogenic VOCs (BVOCs)

In addition to high anthropogenic emissions of aromatics, terrestrial vegetations nearby also released significant amounts of BVOCs (Wu et al., 2020). During the campaign, the concentrations of isoprene at noon were between 0.1 and 1.5 ppb, whereas the range of daily maxima of monoterpenes was 0.05 ~ 2.5 ppb. Hence, a number of oxidation products of BVOCs were detected (Fig. 8 and Fig. S11).

The ion $C_4H_7NO_5I^-$ was the most abundant N-containing organic ion with four or five carbon atoms that were detected in the gas phase. Its daily maxima occurred in the afternoon and correlated moderately with MVK+MACR measured by PTR-ToF-MS (Fig. 8). We consequently assigned $C_4H_7NO_5$ as methylvinylketone nitrates and methacrolein nitrates, which was reported as the second generation of organic nitrates formed from the oxidation of isoprene hydroxynitrates by OH in the presence of NO_X (Fisher et al., 2016; Paulot et al., 2009). Strong correlations were observed between $C_5H_9NO_4I^-$, $C_5H_9NO_5I^-$ and $C_4H_7NO_5I^-$ (r=0.93 and 0.80, respectively), which was in accordance with their similar formation pathways (Jacobs et al., 2014; Wennberg

https://doi.org/10.5194/acp-2020-1187
Preprint. Discussion started: 25 November 2020


Atmospheric Chemistry and Physics Discussions

et al., 2018; Xiong et al., 2015). Hence, we expect these three compounds are common oxidation products of isoprene in the polluted atmosphere. While in aerosol, 2-methylglyceric acid ($C_4H_8O_4$) is a commonly reported oxidation product of isoprene formed in high-NO_X conditions (Surratt et al., 2010). We observed the corresponding ion $C_4H_8O_4I^-$ contributing to OA especially in dry conditions with strong sunlight (Fig. S12). This evidence indicates that isoprene oxidation may contributed to $C_4H_8O_4$, but potential contribution from other sources cannot be ruled out in urban areas.

For the oxidaiton of monoterpenes, we observe reasonable correlation (Fig. S13a, r=0.63) between the ions $C_{10}H_{16}O_3I^-$ and $C_{10}H_{16}O_2H^+$ measured by PTR-ToF-MS. $C_{10}H_{16}O_2H^+$ was attributed to pinonaldehyde formed from the oxidation of monoterpenes (Glasius et al., 2000; Larsen et al., 2001; Mutzel et al., 2016). Therefore, we tentatively assigned $C_{10}H_{16}O_3$ as pinonic acid and its oxocarboxylic acid isomers, which are formed via the oxidation of pinonaldehyde (Fang et al., 2017). $C_8H_{13}NO_6$ also exhibited enhanced gas-phase formation during the day as pinonic acid did. The correlation coefficient of the two compounds (r) was 0.71. In contrast, $C_8H_{11}NO_7$ and $C_{10}H_{15}NO_6$ significantly partitioned to the aerosol phase (F_p=0.68±0.19 and 0.44±0.18, respectively) with maximums at night (Fig. S11), indicative of the role of NO_3 in producing organic nitrates as reported in the literature (Faxon et al., 2018). The time trends of $C_{10}H_{15}NO_6I^-$ in both phases did not resemble well (Fig. S13b). Two possible types of compounds were proposed for $C_{10}H_{15}NO_6$ in previous work: peroxyacetyl nitrate from pinonaldehyde (Faxon et al., 2018; Nah et al., 2016; Schwantes et al., 2020), or organic nitrates (Bean and Hildebrandt Ruiz, 2016; Boyd et al., 2015). We speculate that both compounds contributed to the ion $C_{10}H_{15}NO_6I^-$. As shown in Fig. S14, $C_8H_{12}O_4$ and $C_9H_{14}O_4$ existed mostly in particle-phase (F_p=0.63±0.11 and 0.67±0.10, respectively). We interpreted them as products of monoterpenes via photochemical processes, consistent with the interpretations presented in previous work (Mohr et al., 2013; Mutzel et al., 2015).

3.6 S-containing compounds

https://doi.org/10.5194/acp-2020-1187
Preprint. Discussion started: 25 November 2020


Atmospheric Chemistry and Physics Discussions

Organosulfates are concerned as important components of SOA (Hallquist et al., 2009; Surratt et al., 2007), and they can be detected by iodide anion via proton abstraction (Le Breton et al., 2018b; Lee et al., 2014). We detected the ion $C_2H_3SO_6^-$ with peak concentration in the afternoon (Fig. 9). We attributed $C_2H_3SO_6^-$ to glycolic acid sulfate, as suggested by previous work (Galloway et al., 2009; Liao et al., 2015).

Abundant SO_3I^- was detected in particles, and it correlated well with the ion $C_2H_3SO_6^-$ and sulfates measured by AMS (Fig. 9b and Fig. S15). Previous work indicate that neutral loss of SO_3 during ionization of many organosulfates by cleavage of the S-O bond (Huang et al., 2018). As the result, the SO_3I^- ion from FIGAERO-I-CIMS might be a potential indicator for the total organosulfates. However, more future work is needed for evaluating this possibility.

Other sulfate-related ions during gas-phase modes were also detected including HSO_4^- (sulfuric acid), $CH_3SO_3^-$ (methanesulfonic acid) which were enhanced in the gas phase during daytime, in agreement with the notions of photochemically induced gas-phase oxidation (Brandt and van Eldik, 1995). However, these data were not available for quantification given that these low-volatile species would condense on our long gas sampling inlet. Although it should be noted that measuring sulfuric acid in the gas-phase is difficult and generally requires a "wall-less" source design (Eisele and Tanner, 1993).

3.7 Inorganic compounds

There is a growing interest in N_2O_5 and its product nitryl chloride ($ClNO_2$) because $ClNO_2$ is found to serve as a nocturnal reservoir of Cl radical and reactive nitrogen, and hence enhance the ozone formation next day (Osthoff et al., 2008; Wang et al., 2016). Time series of N_2O_5 and $ClNO_2$ exhibited two patterns. During most of the nights, N_2O_5 started to increase quickly at sunset and lasted for only 2~3 hours, and $ClNO_2$ increased in the meantime and ultimately reached its maximum at night, indicative of local formation of $ClNO_2$. However, sometimes a high level of N_2O_5 did not lead to an increase in $ClNO_2$ (tinted background in Fig. 10a), probably due to the lack of chloride salts on the aerosol (Fig. S16). Other nocturnal species including

https://doi.org/10.5194/acp-2020-1187
Preprint. Discussion started: 25 November 2020


Atmospheric Chemistry and Physics Discussions

455 $ClONO_2$ and Cl_2 were highly correlated with $ClNO_2$ as we expected (r=0.92 and 0.83,
456 respectively), suggesting they had common formation mechanisms (Liu et al., 2017).
457 HNO_3I^- was observed as one of the most abundant species in the mass spectra
458 of FIGAERO-I-CIMS in both gas and particle phase. In the gas phase, the ion HNO_3I^-
459 from I-CIMS has been used to quantify nitric acid (Lee et al., 2018a). The
460 concentrations of gas-phase nitric acid peaked in the afternoon, suggesting
461 photochemistry in the daytime as the dominant source for gas-phase nitric acid.
462 Previous study suggested that HNO_3I^- from particle-phase measurement by
463 FIGAERO-I-CIMS can be indicative of nitrate in the particle phase (Lee et al., 2016).
464 Here, the concentrations of HNO_3I^- in the particle phase were compared with
465 particulate nitrate measured by AMS. Strong correlation was obtained between the two
466 measurements (r=0.93). However, the concentrations measured by FIGAERO-I-CIMS
467 were higher (fitted slope=1.6) than particulate nitrate by AMS, and the discrepancy was
468 larger when organic nitrates concentrations measured by FIGAERO-I-CIMS were
469 higher (Fig. 11c). It suggests that HNO_3I^- in the particle phase from FIGAERO-I-
470 CIMS are formed from thermal-decomposition of both inorganic nitrates (e.g.
471 ammonium nitrate) and organic nitrates.

472 **3.8 Bulk chemical properties of detected organics**

473 The composition of organic compounds detected by FIGAERO-I-CIMS was
474 comprehensively characterized with molecular-level details by depicting the average
475 oxidation states of carbon for closed-shell $C_xH_yO_z$ and $C_xH_yN_{1,2}O_z$ compounds
476 clustered with iodide as a function of carbon number (Fig. 12). The details in calculation
477 of $\overline{OS_C}$ can be found in Section S2 in SI. S-containing compounds were omitted given
478 their negligible variety and concentration compared to the former two chemical classes
479 ($C_xH_yO_z$ and $C_xH_yN_{1,2}O_z$). The average $\overline{OS_C}$ in the particle phase was higher than
480 that in the gas phase at the same carbon number, especially for carbon number between
481 2 and 10. This agrees with our expectation that more oxidized compounds would
482 partition more strongly in aerosol, as indicated by larger fractions in particles (Fp) for
483 higher $\overline{OS_C}$. In addition, the average $\overline{OS_C}$ generally increased for lower carbon

https://doi.org/10.5194/acp-2020-1187
Preprint. Discussion started: 25 November 2020


Atmospheric Chemistry and Physics Discussions

number, as a result of functionalization and fragmentation during VOCs aging. However, there was a notable exception in C5 which had a significantly reduced $\overline{OS_C}$, probably as the result of augmented primary emissions of isoprene. The analysis of the $\overline{OS_C} - n_C$ space indicates that the large number of organic compounds measured by FIGAERO-I-CIMS are useful to characterize the evolution of organic compounds in the atmosphere.

The distributions of carbon number and oxygen number in the organic compounds measured by FIGAERO-I-CIMS were also investigated, as shown in Fig. 13. Most abundant organic compounds measured by FIGAERO-I-CIMS were C2~C3 compounds, which accounted for about 63% of organics in gas-phase and 55% in particle-phase. Organic compounds with carbon numbers over 5 constituted only 9% in the gas phase, while they accounted for 30% in the particle phase. The majority of gaseous organic compounds was associated with less than 4 oxygen atoms. Organic compounds containing 2 and 3 oxygen atoms had the largest contribution in both gas-phase (62%) and particle-phase (44%). $C_xH_yN_{1,2}O_z$ accounted for less than 10% of the total oxygenated organic compounds. In the gas phase, compounds with 5 or 6 oxygen atoms accounted for 51% of $C_xH_yN_{1,2}O_z$, indicative of the high levels of organic nitrates in the urban atmosphere. Nitrophenols also contributed significantly to $C_xH_yN_{1,2}O_z$ compounds, as the fraction of compounds possessing 3 oxygen atoms was 22%. In contrast, in the particle phase, the oxygen number of $C_xH_yN_{1,2}O_z$ distributed relatively evenly, as the fractions of compounds with 3~8 oxygen atoms were similar (between 14% and 19%). Compared to measurements in a forest in the southeastern United States (cf., Table S1 from Lee et al., 2016), the fractions of N-containing organics with less than 5 oxygen atoms were significantly larger in our measurements as a result of higher concentrations of nitro-aromatics.

We further determine the fractions of N-containing organics in total organic compounds as a function of m/z. The observed fractions of N-containing organic compounds were higher for elevated m/z (Fig. 14 and Fig. S17). The gas-phase CHON ions within the m/z range from 250 to 350 Th accounted for about half of the organic compounds in this range. The fractions of CHON ions in particle-phase are somewhat

https://doi.org/10.5194/acp-2020-1187
Preprint. Discussion started: 25 November 2020


Atmospheric Chemistry and Physics Discussions

smaller than those in the gas phase for m/z of 250-350 Th, but are comparable for higher m/z. A possible explanation for this is that functional groups of nitrate and nitro reduce less in vapor pressure for organic compounds than functional groups of carboxylic acid or oxygen-equivalent hydroxyl that without nitrogen atom (Capouet and Müller, 2006; Nannoolal et al., 2008; Pankow and Asher, 2008). Consequently, CHON compounds are generally more volatile than CHO compounds with similar molecular weights.

In the end, we determined the total concentration of N-containing organic compounds in the particle-phase measured by FIGAERO-I-CIMS and compared with the particulate organic nitrates derived from AMS (Fig. 15). Good agreement was achieved when the concentrations of inorganic nitrate were relatively lower, e.g. the period before October 7, 2018. This encouraging result indicates that FIGAERO-I-CIMS is able to capture the variability of organic nitrates in the urban atmosphere, which can be helpful in understanding the sources and formation mechanism of these organic nitrates.

3.9 Organic aerosol measurements

The total concentrations of organic compounds in the particle phase measured by FIGAERO-I-CIMS were determined and compared with measurements of OA by AMS. The total organics measured by FIGAERO-I-CIMS explained 24% of the total OA (Fig. 16a), which is lower than the fractions (~50%) reported previously in boreal and temperate forests (Lopez-Hilfiker et al., 2016; Stark et al., 2017). The lower fractions determined here might be as the result of larger contributions to OA from primary emissions in urban air, which are composed of large number of compounds with little signal in I-CIMS (Zhao et al., 2016). The OA fractions measured by FIGAERO-I-CIMS are higher for aged air with higher O/C ratios in OA determined by AMS (Fig. 16a), consistent with I-CIMS are more sensitive to oxygenated organic compounds with multiple functional groups (Lee et al., 2014; Lopez-Hilfiker et al., 2016). Similar trends were found in Le Breton et al. (2019), in which an acetate source was used. Acetate ions have been reported to selectively ionize highly oxygenated organics as an iodide source do (Aljawhary et al., 2013).

https://doi.org/10.5194/acp-2020-1187
Preprint. Discussion started: 25 November 2020


Atmospheric Chemistry and Physics Discussions

Comparison of the Van Krevelen diagram between FIGAERO-I-CIMS and AMS also provides useful insights on measurement of organic compounds in OA. The Van Krevelen diagram has been used as a tool for analyzing functional groups and OA aging by plotting H/C ratios versus O/C ratios (Heald et al., 2010; Lambe et al., 2012). As shown in Fig. 16a, the data points for bulk OA from FIGAERO-I-CIMS follow the same trend as the data points from AMS. However, the bulk OA measured by FIGAERO-I-CIMS only occupied a much smaller region with the O/C ratio between of 0.7 and 1.0. We further plot all of the organic compounds in the H/C versus O/C space color-coded with their campaign-average concentrations (Fig. S18a). We observe most particle-phase concentrations measured by FIGAERO-I-CIMS distributed across the zone between the slope of 0 and -1.0. These observations provide additional evidence that FIGAERO-I-CIMS may only measure the more oxidized organic compounds in OA.

The correlation coefficients between the particle-phase concentrations of various compounds by FIGAERO-I-CIMS and OA by AMS are calculated (Fig. S18b). The correlation coefficients are small for ions below m/z 200, as these ions contribute little to organic aerosol. Moderate and strong correlation were observed for the ions between m/z 200 and m/z 400, implying that organic compounds with molecular weight of 100-300 g/mol may account for significant fractions in organic aerosol. The correlation coefficients start to decrease for ions above m/z 400, likely due to decomposition during heating or partially evaporation from FIGAERO filter for these high-molecular weight compounds.

4 Conclusions

We deployed a FIGAERO-I-CIMS instrument to measure oxygenated organic compounds in both gas phase and particle phase at a representative urban site in China. The mass spectra from the FIGAERO-I-CIMS from the measurements was systematically interpreted. We detected high concentrations of several monosaccharide species (e.g., levoglucosan) potentially emitted from biomass burning, which also contributed to the enhancement of multiple nitro-aromatic species. Photochemistry was

https://doi.org/10.5194/acp-2020-1187
Preprint. Discussion started: 25 November 2020


Atmospheric Chemistry and Physics Discussions

572 also identified as a strong source of nitro-aromatics. Low-molecular-weight organic
573 acids were mainly observed in the gas phase, and observations support daytime
574 photochemistry as the dominant source. Various oxidation products of BVOCs were
575 detected in both gas and particle phase, reflecting the role of NO_X in the oxidation of
576 BVOC species. Local formation of nitryl chloride was observed, highlighting the
577 potential importance of nighttime chemistry in the urban region.

578 Our measurements show that oxygenated organic compounds dominated the
579 majority of detected species by FIGAERO-I-CIMS, in which CHO and CHON
580 compounds both accounted for significant fractions. Nitrogen-containing organic
581 compounds occupied a significant fraction of the total signal in both gas and particle
582 phases, with elevated fractions at higher molecular weights. The most abundant organic
583 compounds were formic acid and multifunctional organics containing 3~5 oxygen
584 atoms. Organic compounds containing 2 or 3 carbon atoms accounted for over half of
585 total organics in both gas- and particle phase measured by FIGAERO-I-CIMS. During
586 the campaign, the FIGAERO-I-CIMS measurements explained 24% of OA measured
587 by AMS, however the fractions are higher for measurements of more aged organic
588 aerosol in the urban atmosphere. This evidence, along with the analysis of the Van
589 Krevelen plot, indicate that FIGAERO-I-CIMS were measuring the more oxidized
590 fraction of OA in the urban air.

591

592 ## Acknowledgement

593 This work was supported by the National Key R&D Plan of China (grant No.
594 2019YFE0106300, 2018YFC0213904, 2016YFC0202206), the National Natural
595 Science Foundation of China (grant No. 41877302), Guangdong Natural Science
596 Funds for Distinguished Young Scholar (grant No. 2018B030306037), Guangdong
597 Provincial Key R&D Plan (grant No. 2019B110206001), Guangdong Soft Science
598 Research Program (grant No. 2019B101001005) and Guangdong Innovative and
599 Entrepreneurial Research Team Program (grant No. 2016ZT06N263). This work was
600 also supported by Special Fund Project for Science and Technology Innovation Strategy

https://doi.org/10.5194/acp-2020-1187
Preprint. Discussion started: 25 November 2020

601 of Guangdong Province (Grant No.2019B121205004). Weiwei Hu and Wei Chen were
602 supported by National Natural Science Foundation of China (41875156).

603 Data availability

604 The more detailed data can be provided by contacting the corresponding authors.

605 Author contributions

606 BY and MS designed the research. CSY, YL, ZLW, TGL, WWH, WC, CHW,
607 CMW, SH, JPQ, BLW, CW, WS, XMW, ZYZ, XMW contributed to data collection.
608 CSY performed the data analysis with contributions from WWH and WC. CSY and
609 BY prepared the manuscript with contributions from JEK and other authors. All the
610 authors reviewed the manuscript.

611 Competing interest

612 The authors declare that they have no conflicts of interest.

613

614

615 References

616 Aiken, A. C., DeCarlo, P. F. and Jimenez, J. L.: Elemental Analysis of Organic
617 Species with Electron Ionization High-Resolution Mass Spectrometry, Anal. Chem.,
618 79(21), 8350–8358, doi:10.1021/ac071150w, 2007.
619 Aljawhary, D., Lee, A. K. Y. and Abbatt, J. P. D.: High-resolution chemical
620 ionization mass spectrometry (ToF-CIMS): Application to study SOA composition
621 and processing, Atmos. Meas. Tech., 6(11), 3211–3224, doi:10.5194/amt-6-3211-
622 2013, 2013.
623 Bean, J. K. and Hildebrandt Ruiz, L.: Gas-particle partitioning and hydrolysis of
624 organic nitrates formed from the oxidation of alpha-pinene in environmental chamber
625 experiments, Atmos. Chem. Phys., 16(4), 2175–2184, doi:10.5194/acp-16-2175-2016,
626 2016.

https://doi.org/10.5194/acp-2020-1187
Preprint. Discussion started: 25 November 2020


Atmospheric Chemistry and Physics Discussions

627 Berndt, T., Scholz, W., Mentler, B., Fischer, L., Herrmann, H., Kulmala, M. and
628 Hansel, A.: Accretion Product Formation from Self- and Cross-Reactions of RO2
629 Radicals in the Atmosphere, Angew. Chemie Int. Ed., 57(14), 3820–3824,
630 doi:10.1002/anie.201710989, 2018.
631 Berndt, T., Hyttinen, N., Herrmann, H. and Hansel, A.: First oxidation products from
632 the reaction of hydroxyl radicals with isoprene for pristine environmental conditions,
633 Commun. Chem., 2(1), 1–10, doi:10.1038/s42004-019-0120-9, 2019.
634 Bertram, T. H., Thornton, J. A. and Riedel, T. P.: An experimental technique for the
635 direct measurement of N2O5 reactivity on ambient particles, Atmos. Meas. Tech.,
636 2(1), 231–242, doi:10.5194/amt-2-231-2009, 2009.
637 Bertram, T. H., Kimmel, J. R., Crisp, T. A., Ryder, O. S., Yatavelli, R. L. N.,
638 Thornton, J. A., Cubison, M. J., Gonin, M. and Worsnop, D. R.: A field-deployable,
639 chemical ionization time-of-flight mass spectrometer, Atmos. Meas. Tech., 4(7),
640 1471–1479, doi:10.5194/amt-4-1471-2011, 2011.
641 Bhattarai, H., Saikawa, E., Wan, X., Zhu, H., Ram, K., Gao, S., Kang, S., Zhang, Q.,
642 Zhang, Y., Wu, G., Wang, X., Kawamura, K., Fu, P. and Cong, Z.: Levoglucosan as a
643 tracer of biomass burning: Recent progress and perspectives, Atmos. Res.,
644 220(November 2018), 20–33, doi:10.1016/j.atmosres.2019.01.004, 2019.
645 Boyd, C. M., Sanchez, J., Xu, L., Eugene, A. J., Nah, T., Tuet, W. Y., Guzman, M. I.
646 and Ng, N. L.: Secondary organic aerosol formation from the β-pinene+NO3 system:
647 effect of humidity and peroxy radical fate, Atmos. Chem. Phys., 15(13), 7497–7522,
648 doi:10.5194/acp-15-7497-2015, 2015.
649 Brandt, C. and van Eldik, R.: Transition Metal-Catalyzed Oxidation of Sulfur(IV)
650 Oxides. Atmospheric-Relevant Processes and Mechanisms, Chem. Rev., 95(1), 119–
651 190, doi:10.1021/cr00033a006, 1995.
652 Brege, M., Paglione, M., Gilardoni, S., Decesari, S., Cristina Facchini, M. and
653 Mazzoleni, L. R.: Molecular insights on aging and aqueous-phase processing from
654 ambient biomass burning emissions-influenced Po Valley fog and aerosol, Atmos.
655 Chem. Phys., 18(17), 13197–13214, doi:10.5194/acp-18-13197-2018, 2018.
656 Le Breton, M., Hallquist, A. M., Pathak, R. K., Simpson, D., Wang, Y., Johansson, J.,

https://doi.org/10.5194/acp-2020-1187
Preprint. Discussion started: 25 November 2020


Atmospheric Chemistry and Physics Discussions

657 Zheng, J., Yang, Y., Shang, D., Wang, H., Liu, Q., Chan, C., Wang, T., Bannan, T. J.,
658 Priestley, M., Percival, C. J., Shallcross, D. E., Lu, K., Guo, S., Hu, M. and Hallquist,
659 M.: Chlorine oxidation of VOCs at a semi-rural site in Beijing: significant chlorine
660 liberation from ClNO2 and subsequent gas- and particle-phase Cl-VOC production,
661 Atmos. Chem. Phys., 18(17), 13013–13030, doi:10.5194/acp-18-13013-2018, 2018a.
662 Le Breton, M., Wang, Y., Hallquist, Å. M., Pathak, R. K., Zheng, J., Yang, Y., Shang,
663 D., Glasius, M., Bannan, T. J., Liu, Q., Chan, C. K., Percival, C. J., Zhu, W., Lou, S.,
664 Topping, D., Wang, Y., Yu, J., Lu, K., Guo, S., Hu, M. and Hallquist, M.: Online gas-
665 and particle-phase measurements of organosulfates, organosulfonates and nitrooxy
666 organosulfates in Beijing utilizing a FIGAERO ToF-CIMS, Atmos. Chem. Phys.,
667 18(14), 10355–10371, doi:10.5194/acp-18-10355-2018, 2018b.
668 Le Breton, M., Psichoudaki, M., Hallquist, M., Watne, Å. K., Lutz, A. and Hallquist,
669 Å. M.: Application of a FIGAERO ToF CIMS for on-line characterization of real-
670 world fresh and aged particle emissions from buses, Aerosol Sci. Technol., 53(3),
671 244–259, doi:10.1080/02786826.2019.1566592, 2019.
672 Canagaratna, M. R., Jimenez, J. L., Kroll, J. H., Chen, Q., Kessler, S. H., Massoli, P.
673 and Ruiz, L. H.: Elemental ratio measurements of organic compounds using aerosol
674 mass spectrometry: characterization, improved calibration, and implications, Atmos.
675 Chem. Phys., 15, 253–272, doi:10.5194/acp-15-253-2015, 2015.
676 Capouet, M. and Müller, J. F.: A group contribution method for estimating the vapour
677 pressures of α-pinene oxidation products, Atmos. Chem. Phys., 6(6), 1455–1467,
678 doi:10.5194/acp-6-1455-2006, 2006.
679 Carlton, A. G., Turpin, B. J., Altieri, K. E., Seitzinger, S., Reff, A., Lim, H.-J. and
680 Ervens, B.: Atmospheric oxalic acid and SOA production from glyoxal: Results of
681 aqueous photooxidation experiments, Atmos. Environ., 41(35), 7588–7602,
682 doi:10.1016/j.atmosenv.2007.05.035, 2007.
683 Carslaw, N.: A mechanistic study of limonene oxidation products and pathways
684 following cleaning activities, Atmos. Environ., 80, 507–513,
685 doi:https://doi.org/10.1016/j.atmosenv.2013.08.034, 2013.
686 Chen, H. and Finlayson-Pitts, B. J.: New Particle Formation from Methanesulfonic

https://doi.org/10.5194/acp-2020-1187
Preprint. Discussion started: 25 November 2020


Atmospheric Chemistry and Physics Discussions

687 Acid and Amines/Ammonia as a Function of Temperature, Environ. Sci. Technol.,
688 51(1), 243–252, doi:10.1021/acs.est.6b04173, 2017.
689 Chen, J., Wenger, J. C. and Venables, D. S.: Near-Ultraviolet Absorption Cross
690 Sections of Nitrophenols and Their Potential Influence on Tropospheric Oxidation
691 Capacity, J. Phys. Chem. A, 115(44), 12235–12242, doi:10.1021/jp206929r, 2011.
692 Cubison, M. J., Ortega, A. M., Hayes, P. L., Farmer, D. K., Day, D., Lechner, M. J.,
693 Brune, W. H., Apel, E., Diskin, G. S., Fisher, J. A., Fuelberg, H. E., Hecobian, A.,
694 Knapp, D. J., Mikoviny, T., Riemer, D., Sachse, G. W., Sessions, W., Weber, R. J.,
695 Weinheimer, A. J., Wisthaler, A. and Jimenez, J. L.: Effects of aging on organic
696 aerosol from open biomass burning smoke in aircraft and laboratory studies, Atmos.
697 Chem. Phys., 11(23), 12049–12064, doi:10.5194/acp-11-12049-2011, 2011.
698 Edwards, P. M., Brown, S. S., Roberts, J. M., Ahmadov, R., Banta, R. M., DeGouw,
699 J. A., Dubé, W. P., Field, R. A., Flynn, J. H., Gilman, J. B., Graus, M., Helmig, D.,
700 Koss, A., Langford, A. O., Lefer, B. L., Lerner, B. M., Li, R., Li, S. M., McKeen, S.
701 A., Murphy, S. M., Parrish, D. D., Senff, C. J., Soltis, J., Stutz, J., Sweeney, C.,
702 Thompson, C. R., Trainer, M. K., Tsai, C., Veres, P. R., Washenfelder, R. A.,
703 Warneke, C., Wild, R. J., Young, C. J., Yuan, B. and Zamora, R.: High winter ozone
704 pollution from carbonyl photolysis in an oil and gas basin, Nature, 514(7522), 351–
705 354, doi:10.1038/nature13767, 2014.
706 Eger, P. G., Schuladen, J., Sobanski, N., Fischer, H., Karu, E., Williams, J., Riva, M.,
707 Zha, Q., Ehn, M., Quéléver, L. L. J., Schallhart, S., Lelieveld, J. and Crowley, J. N.:
708 Pyruvic acid in the boreal forest: gas-phase mixing ratios and impact on radical
709 chemistry, Atmos. Chem. Phys., 20(6), 3697–3711, doi:10.5194/acp-20-3697-2020,
710 2020.
711 Eisele, F. L. and Tanner, D. J.: Measurement of the gas phase concentration of
712 H2SO4 and methane sulfonic acid and estimates of H2SO4 production and loss in the
713 atmosphere, J. Geophys. Res. Atmos., 98(D5), 9001–9010, doi:10.1029/93JD00031,
714 1993.
715 Fang, W., Gong, L. and Sheng, L.: Online analysis of secondary organic aerosols
716 from OH-initiated photooxidation and ozonolysis of α-pinene, β-pinene, Δ3-carene

https://doi.org/10.5194/acp-2020-1187
Preprint. Discussion started: 25 November 2020


Atmospheric Chemistry and Physics Discussions

and d-limonene by thermal desorption-photoionisation aerosol mass spectrometry, Environ. Chem., 14(2), 75–90, doi:10.1071/EN16128, 2017.

Faxon, C., Hammes, J., Pathak, R. K. and Hallquist, M.: Characterization of organic nitrate constituents of secondary organic aerosol (SOA) from nitrate-radical-initiated oxidation of limonene using High-Resolution Chemical Ionization Mass Spectrometry, Atmos. Chem. Phys., 18, 5467–5481, doi:10.5194/acp-2017-584, 2018.

Fisher, J. A., Jacob, D. J., Travis, K. R., Kim, P. S., Marais, E. A., Chan Miller, C., Yu, K., Zhu, L., Yantosca, R. M. and Sulprizio, M. P.: Organic Nitrate Chemistry and its Implications for Nitrogen Budgets in an Isoprene- and Monoterpene-Rich Atmosphere: Constraints from Aircraft (SEAC4RS) and Ground-Based (SOAS) Observations in the Southeast US, Atmos. Chem. Phys., 16, 5969 [online] Available from: https://www.atmos-chem-phys.net/16/5969/2016/acp-16-5969-2016.pdf, 2016.

Fountoukis, C. and Nenes, A.: ISORROPIA II: a computationally efficient thermodynamic equilibrium model for K+–Ca2+–Mg2+–NH+ 4 –Na+–SO2− 4 –NO− 3 –Cl−–H2O aerosols, Atmos. Chem. Phys., 7(17), 4639–4659, doi:10.5194/acp-7-4639-2007, 2007.

Fry, J. L., Draper, D. C., Zarzana, K. J., Campuzano-Jost, P., Day, D. A., Jimenez, J. L., Brown, S. S., Cohen, R. C., Kaser, L., Hansel, A., Cappellin, L., Karl, T., Hodzic Roux, A., Turnipseed, A., Cantrell, C., Lefer, B. L., Grossberg, N., Farmer, D. K. and Jimenez, J. L.: Observations of gas- and aerosol-phase organic nitrates at BEACHON-RoMBAS 2011, Atmos. Chem. Phys., 13(17), 8585–8605, doi:10.5194/acp-13-8585-2013, 2013.

Galloway, M. M., Chhabra, P. S., Chan, A. W. H., Surratt, J. D., Flagan, R. C., Seinfeld, J. H. and Keutsch, F. N.: Glyoxal uptake on ammonium sulphate seed aerosol: reaction products and reversibility of uptake under dark and irradiated conditions, Atmos. Chem. Phys., 9(10), 3331–3345, doi:10.5194/acp-9-3331-2009, 2009.

Gaston, C. J., Lopez-Hilfiker, F. D., Whybrew, L. E., Hadley, O., McNair, F., Gao, H., Jaffe, D. A. and Thornton, J. A.: Online molecular characterization of fine particulate matter in Port Angeles, WA: Evidence for a major impact from residential

https://doi.org/10.5194/acp-2020-1187
Preprint. Discussion started: 25 November 2020

747 wood smoke, Atmos. Environ., 138, 99–107, doi:10.1016/j.atmosenv.2016.05.013,
748 2016.
749 Glasius, M., Lahaniati, M., Calogirou, A., Di Bella, D., Jensen, N. R., Hjorth, J.,
750 Kotzias, D. and Larsen, B. R.: Carboxylic acids in secondary aerosols from oxidation
751 of cyclic monoterpenes by ozone, Environ. Sci. Technol., 34(6), 1001–1010,
752 doi:10.1021/es990445r, 2000.
753 Gondwe, M., Krol, M., Gieskes, W., Klaassen, W. and de Baar, H.: The contribution
754 of ocean-leaving DMS to the global atmospheric burdens of DMS, MSA, SO2, and
755 NSS SO4=, Global Biogeochem. Cycles, 17(2), doi:10.1029/2002GB001937, 2003.
756 de Gouw, J. A., Middlebrook, A. M., Warneke, C., Goldan, P. D., Kuster, W. C.,
757 Roberts, J. M., Fehsenfeld, F. C., Worsnop, D. R., Canagaratna, M. R., Pszenny, A.
758 A. P., Keene, W. C., Marchewka, M., Bertman, S. B. and Bates, T. S.: Budget of
759 organic carbon in a polluted atmosphere: Results from the New England Air Quality
760 Study in 2002, J. Geophys. Res. D Atmos., 110(16), 1–22,
761 doi:10.1029/2004JD005623, 2005.
762 de Gouw, J. A., Gilman, J. B., Kim, S. W., Alvarez, S. L., Dusanter, S., Graus, M.,
763 Griffith, S. M., Isaacman-VanWertz, G., Kuster, W. C., Lefer, B. L., Lerner, B. M.,
764 McDonald, B. C., Rappenglück, B., Roberts, J. M., Stevens, P. S., Stutz, J., Thalman,
765 R., Veres, P. R., Volkamer, R., Warneke, C., Washenfelder, R. A. and Young, C. J.:
766 Chemistry of Volatile Organic Compounds in the Los Angeles Basin: Formation of
767 Oxygenated Compounds and Determination of Emission Ratios, J. Geophys. Res.
768 Atmos., 123(4), 2298–2319, doi:10.1002/2017JD027976, 2018.
769 Guo, H., Xu, L., Bougiatioti, A., Cerully, K. M., Capps, S. L., Hite, J. R., Carlton, A.
770 G., Lee, S. H., Bergin, M. H., Ng, N. L., Nenes, A. and Weber, R. J.: Fine-particle
771 water and pH in the southeastern United States, Atmos. Chem. Phys., 15(9), 5211–
772 5228, doi:10.5194/acp-15-5211-2015, 2015.
773 Hallquist, M., Wenger, J. C., Baltensperger, U., Rudich, Y., Simpson, D., Claeys, M.,
774 Dommen, J., Donahue, N. M., George, C., Goldstein, a. H., Hamilton, J. F.,
775 Herrmann, H., Hoffmann, T., Iinuma, Y., Jang, M., Jenkin, M. E., Jimenez, J. L.,
776 Kiendler-Scharr, a., Maenhaut, W., McFiggans, G., Mentel, T. F., Monod, a.,

https://doi.org/10.5194/acp-2020-1187
Preprint. Discussion started: 25 November 2020


Atmospheric Chemistry and Physics Discussions

777 Prévôt, a. S. H., Seinfeld, J. H., Surratt, J. D., Szmigielski, R. and Wildt, J.: The
778 formation, properties and impact of secondary organic aerosol: current and emerging
779 issues, Atmos. Chem. Phys., 9(14), 5155–5236, doi:10.5194/acp-9-5155-2009, 2009.
780 Harrison, M. A. J., Barra, S., Borghesi, D., Vione, D., Arsene, C. and Iulian Olariu,
781 R.: Nitrated phenols in the atmosphere: a review, Atmos. Environ., 39(2), 231–248,
782 doi:https://doi.org/10.1016/j.atmosenv.2004.09.044, 2005.
783 He, Q.-F., Ding, X., Wang, X.-M., Yu, J.-Z., Fu, X.-X., Liu, T.-Y., Zhang, Z., Xue, J.,
784 Chen, D.-H., Zhong, L.-J. and Donahue, N. M.: Organosulfates from Pinene and
785 Isoprene over the Pearl River Delta, South China: Seasonal Variation and Implication
786 in Formation Mechanisms, Environ. Sci. Technol., 48(16), 9236–9245,
787 doi:10.1021/es501299v, 2014.
788 Heald, C. L., Kroll, J. H., Jimenez, J. L., Docherty, K. S., Decarlo, P. F., Aiken, A. C.,
789 Chen, Q., Martin, S. T., Farmer, D. K. and Artaxo, P.: A simplified description of the
790 evolution of organic aerosol composition in the atmosphere, Geophys. Res. Lett.,
791 37(8), doi:10.1029/2010GL042737, 2010.
792 Hodzic, A., Jimenez, J. L., Madronich, S., Canagaratna, M. R., Decarlo, P. F.,
793 Kleinman, L. and Fast, J.: Modeling organic aerosols in a megacity: Potential
794 contribution of semi-volatile and intermediate volatility primary organic compounds
795 to secondary organic aerosol formation, Atmos. Chem. Phys., 10(12), 5491–5514,
796 doi:10.5194/acp-10-5491-2010, 2010.
797 Hu, W., Hu, M., Hu, W., Jimenez, J. L., Yuan, B., Chen, W., Wang, M., Wu, Y.,
798 Chen, C., Wang, Z., Peng, J., Zeng, L. and Shao, M.: Chemical composition, sources,
799 and aging process of submicron aerosols in Beijing: Contrast between summer and
800 winter, J. Geophys. Res. Atmos., 121(4), 1955–1977, doi:10.1002/2015JD024020,
801 2016.
802 Hu, W., Day, D. A., Campuzano-Jost, P., Nault, B. A., Park, T., Lee, T., Croteau, P.,
803 Canagaratna, M. R., Jayne, J. T., Worsnop, D. R. and Jimenez, J. L.: Evaluation of the
804 new capture vaporizer for aerosol mass spectrometers: Characterization of organic
805 aerosol mass spectra, Aerosol Sci. Technol., 52(7), 725–739,
806 doi:10.1080/02786826.2018.1454584, 2018.

https://doi.org/10.5194/acp-2020-1187
Preprint. Discussion started: 25 November 2020

Huang, R.-J., Cao, J., Chen, Y., Yang, L., Shen, J., You, Q., Wang, K., Lin, C., Xu, W., Gao, B., Li, Y., Chen, Q., Hoffmann, T., O'Dowd, C. D., Bilde, M. and Glasius, M.: Organosulfates in atmospheric aerosol: synthesis and quantitative analysis of PM2.5 from Xi'an, northwestern China, Atmos. Meas. Tech., 11(6), 3447–3456, doi:10.5194/amt-11-3447-2018, 2018.

Huang, R. J., Zhang, Y., Bozzetti, C., Ho, K. F., Cao, J. J., Han, Y., Daellenbach, K. R., Slowik, J. G., Platt, S. M., Canonaco, F., Zotter, P., Wolf, R., Pieber, S. M., Bruns, E. A., Crippa, M., Ciarelli, G., Piazzalunga, A., Schwikowski, M., Abbaszade, G., Schnelle-Kreis, J., Zimmermann, R., An, Z., Szidat, S., Baltensperger, U., El Haddad, I. and Prévôt, A. S. H.: High secondary aerosol contribution to particulate pollution during haze events in China, Nature, 514(7521), 218–222, doi:10.1038/nature13774, 2015.

Huang, W., Saathoff, H., Shen, X., Ramisetty, R., Leisner, T. and Mohr, C.: Chemical Characterization of Highly Functionalized Organonitrates Contributing to Night-Time Organic Aerosol Mass Loadings and Particle Growth, Environ. Sci. Technol., 53(3), 1165–1174, doi:10.1021/acs.est.8b05826, 2019.

Hunter, J. F., Day, D. A., Palm, B. B., Yatavelli, R. L. N., Chan, A. W. H., Kaser, L., Cappellin, L., Hayes, P. L., Cross, E. S., Carrasquillo, A. J., Campuzano-Jost, P., Stark, H., Zhao, Y., Hohaus, T., Smith, J. N., Hansel, A., Karl, T., Goldstein, A. H., Guenther, A., Worsnop, D. R., Thornton, J. A., Heald, C. L., Jimenez, J. L. and Kroll, J. H.: Comprehensive characterization of atmospheric organic carbon at a forested site, Nat. Geosci., 10(10), 748–753, doi:10.1038/NGEO3018, 2017.

Hyttinen, N., Otkjær, R. V., Iyer, S., Kjaergaard, H. G., Rissanen, M. P., Wennberg, P. O. and Kurtén, T.: Computational Comparison of Different Reagent Ions in the Chemical Ionization of Oxidized Multifunctional Compounds, J. Phys. Chem. A, 122(1), 269–279, doi:10.1021/acs.jpca.7b10015, 2018.

Isaacman-VanWertz, G., Massoli, P., O'Brien, R., Lim, C., Franklin, J., Moss, J., Hunter, J., Nowak, J., Canagaratna, M., Misztal, P., Arata, C., Roscioli, J., Herndon, S., Onasch, T., Lambe, A., Jayne, J., Su, L., Knopf, D., Goldstein, A., Worsnop, D. and Kroll, J.: Chemical evolution of atmospheric organic carbon over multiple

https://doi.org/10.5194/acp-2020-1187
Preprint. Discussion started: 25 November 2020


Atmospheric Chemistry and Physics Discussions

837 generations of oxidation, Nat. Chem., 10(4), 462–468, doi:10.1038/s41557-018-0002-
838 2, 2018.
839 Iyer, S., Lopez-Hilfiker, F., Lee, B. H., Thornton, J. A. and Kurtén, T.: Modeling the
840 Detection of Organic and Inorganic Compounds Using Iodide-Based Chemical
841 Ionization, J. Phys. Chem. A, 120(4), 576–587, doi:10.1021/acs.jpca.5b09837, 2016.
842 Jacobs, M. I., Burke, W. J. and Elrod, M. J.: Kinetics of the Reactions of Isoprene-
843 Derived Hydroxynitrates: Gas Phase Epoxide Formation and Solution Phase
844 Hydrolysis, Atmos. Chem. Phys., 14, 8933, 2014.
845 Karl, T., Striednig, M., Graus, M., Hammerle, A. and Wohlfahrt, G.: Urban flux
846 measurements reveal a large pool of oxygenated volatile organic compound
847 emissions, Proc. Natl. Acad. Sci., 201714715, doi:10.1073/pnas.1714715115, 2018.
848 Kawamura, K. and Bikkina, S.: A review of dicarboxylic acids and related
849 compounds in atmospheric aerosols: Molecular distributions, sources and
850 transformation, Atmos. Res., 170, 140–160,
851 doi:https://doi.org/10.1016/j.atmosres.2015.11.018, 2016.
852 Kawamura, K., Kasukabe, H. and Barrie, L. A.: Source and reaction pathways of
853 dicarboxylic acids, ketoacids and dicarbonyls in arctic aerosols: One year of
854 observations, Atmos. Environ., 30(10), 1709–1722, doi:https://doi.org/10.1016/1352-
855 2310(95)00395-9, 1996.
856 Kong, X., Salvador, C. M., Carlsson, S., Pathak, R., Davidsson, K. O., Le Breton, M.,
857 Gaita, S. M., Mitra, K., Hallquist, Å. M., Hallquist, M. and Pettersson, J. B. C.:
858 Molecular characterization and optical properties of primary emissions from a
859 residential wood burning boiler, Sci. Total Environ., 754, 142143,
860 doi:https://doi.org/10.1016/j.scitotenv.2020.142143, 2021.
861 Kroll, J. H. and Seinfeld, J. H.: Chemistry of secondary organic aerosol: Formation
862 and evolution of low-volatility organics in the atmosphere, Atmos. Environ., 42(16),
863 3593–3624, doi:10.1016/j.atmosenv.2008.01.003, 2008.
864 Lambe, A. T., Onasch, T. B., Croasdale, D. R., Wright, J. P., Martin, A. T., Franklin,
865 J. P., Massoli, P., Kroll, J. H., Canagaratna, M. R., Brune, W. H., Worsnop, D. R. and
866 Davidovits, P.: Transitions from functionalization to fragmentation reactions of

https://doi.org/10.5194/acp-2020-1187
Preprint. Discussion started: 25 November 2020

867 laboratory Secondary Organic Aerosol (SOA) generated from the OH oxidation of
868 alkane precursors, Environ. Sci. Technol., 46(10), 5430–5437,
869 doi:10.1021/es300274t, 2012.
870 Larsen, B. R., Di Bella, D., Glasius, M., Winterhalter, R., Jensen, N. R. and Hjorth, J.:
871 Gas-phase OH oxidation of monoterpenes: Gaseous and particulate products, J.
872 Atmos. Chem., 38(3), 231–276, doi:10.1023/A:1006487530903, 2001.
873 Lee, B. H., Lopez-Hilfiker, F. D., Mohr, C., Kurtén, T., Worsnop, D. R. and
874 Thornton, J. A.: An iodide-adduct high-resolution time-of-flight chemical-ionization
875 mass spectrometer: Application to atmospheric inorganic and organic compounds,
876 Environ. Sci. Technol., 48(11), 6309–6317, doi:10.1021/es500362a, 2014.
877 Lee, B. H., Mohr, C., Lopez-Hilfiker, F. D., Lutz, A., Hallquist, M., Lee, L., Romer,
878 P., Cohen, R. C., Iyer, S., Kurtén, T., Hu, W., Day, D. A., Campuzano-Jost, P.,
879 Jimenez, J. L., Xu, L., Ng, N. L., Guo, H., Weber, R. J., Wild, R. J., Brown, S. S.,
880 Koss, A., de Gouw, J., Olson, K., Goldstein, A. H., Seco, R., Kim, S., McAvey, K.,
881 Shepson, P. B., Starn, T., Baumann, K., Edgerton, E. S., Liu, J., Shilling, J. E., Miller,
882 D. O., Brune, W., Schobesberger, S., D'Ambro, E. L. and Thornton, J. A.: Highly
883 functionalized organic nitrates in the southeast United States: Contribution to
884 secondary organic aerosol and reactive nitrogen budgets, Proc. Natl. Acad. Sci.,
885 113(6), 1516–1521, doi:10.1073/pnas.1508108113, 2016.
886 Lee, B. H., Lopez-hilfiker, F. D., Veres, P. R., Mcduffie, E. E., Fibiger, D. L.,
887 Tamara, L. and Thornton, J. A.: Flight deployment of a high-resolution time-of-flight
888 chemical ionization mass spectrometer : observations of reactive halogen and nitrogen
889 oxide species, , doi:10.1029/2017JD028082, 2018a.
890 Lee, B. H., Lopez-Hilfiker, F. D., D'Ambro, E. L., Zhou, P., Boy, M., Petäjä, T., Hao,
891 L., Virtanen, A. and Thornton, J. A.: Semi-volatile and highly oxygenated gaseous
892 and particulate organic compounds observed above a boreal forest canopy, Atmos.
893 Chem. Phys., 18(15), 11547–11562, doi:10.5194/acp-18-11547-2018, 2018b.
894 Liao, J., Froyd, K. D., Murphy, D. M., Keutsch, F. N., Yu, G., Wennberg, P. O., St
895 Clair, J. M., Crounse, J. D., Wisthaler, A., Mikoviny, T., Jimenez, J. L., Campuzano-
896 Jost, P., Day, D. A., Hu, W., Ryerson, T. B., Pollack, I. B., Peischl, J., Anderson, B.

https://doi.org/10.5194/acp-2020-1187
Preprint. Discussion started: 25 November 2020


Atmospheric Chemistry and Physics Discussions

E., Ziemba, L. D., Blake, D. R., Meinardi, S. and Diskin, G.: Airborne measurements of organosulfates over the continental U.S, J. Geophys. Res. Atmos. JGR, 120(7), 2990–3005, doi:10.1002/2014JD022378, 2015.

Lim, H.-J., Carlton, A. G. and Turpin, B. J.: Isoprene Forms Secondary Organic Aerosol through Cloud Processing: Model Simulations, Environ. Sci. Technol., 39(12), 4441–4446, doi:10.1021/es048039h, 2005.

Liu, X., Qu, H., Huey, L. G., Wang, Y., Sjostedt, S., Zeng, L., Lu, K., Wu, Y., Hu, M., Shao, M., Zhu, T. and Zhang, Y.: High Levels of Daytime Molecular Chlorine and Nitryl Chloride at a Rural Site on the North China Plain, Environ. Sci. Technol., 51(17), 9588–9595, doi:10.1021/acs.est.7b03039, 2017.

Liu, Z., Wang, Y., Gu, D., Zhao, C., Huey, L. G., Stickel, R., Liao, J., Shao, M., Zhu, T., Zeng, L., Amoroso, A., Costabile, F., Chang, C. C. and Liu, S. C.: Summertime photochemistry during CAREBeijing-2007: ROxbudgets and O3 formation, Atmos. Chem. Phys., 12(16), 7737–7752, doi:10.5194/acp-12-7737-2012, 2012.

Lopez-Hilfiker, F. D., Mohr, C., Ehn, M., Rubach, F., Kleist, E., Wildt, J., Mentel, T. F., Lutz, A., Hallquist, M., Worsnop, D. and Thornton, J. A.: A novel method for online analysis of gas and particle composition: description and evaluation of a Filter Inlet for Gases and AEROsols (FIGAERO), Atmos. Meas. Tech., 7(4), 983–1001, doi:10.5194/amt-7-983-2014, 2014.

Lopez-Hilfiker, F. D., Mohr, C., Ehn, M., Rubach, F., Kleist, E., Wildt, J., Mentel, T. F. and Carrasquillo, A. J.: Phase partitioning and volatility of secondary organic aerosol components formed from α -pinene ozonolysis and OH oxidation : the importance of accretion products and other low volatility compounds, Atmos. Chem. Phys., 15, 7765–7776, doi:10.5194/acp-15-7765-2015, 2015.

Lopez-Hilfiker, F. D., Iyer, S., Mohr, C., Lee, B. H., Ambro, E. L. D., Kurtén, T. and Thornton, J. A.: Constraining the sensitivity of iodide adduct chemical ionization mass spectrometry to multifunctional organic molecules using the collision limit and thermodynamic stability of iodide ion adducts, Atmos. Meas. Tech., 9, 1505–1512, doi:10.5194/amt-9-1505-2016, 2016.

Massoli, P., Stark, H., Canagaratna, M. R., Krechmer, J. E., Xu, L., Ng, N. L.,

https://doi.org/10.5194/acp-2020-1187
Preprint. Discussion started: 25 November 2020


Atmospheric Chemistry and Physics Discussions

927 Mauldin, R. L., Yan, C., Kimmel, J., Misztal, P. K., Jimenez, J. L., Jayne, J. T. and
928 Worsnop, D. R.: Ambient Measurements of Highly Oxidized Gas-Phase Molecules
929 during the Southern Oxidant and Aerosol Study (SOAS) 2013, ACS Earth Sp. Chem.,
930 2(7), 653–672, doi:10.1021/acsearthspacechem.8b00028, 2018.
931 Mattila, J. M., Brophy, P., Kirkland, J., Hall, S., Ullmann, K., Fischer, E. V., Brown,
932 S., McDuffie, E., Tevlin, A. and Farmer, D. K.: Tropospheric sources and sinks of
933 gas-phase acids in the Colorado Front Range, Atmos. Chem. Phys., 18(16), 12315–
934 12327, doi:10.5194/acp-18-12315-2018, 2018.
935 Mehra, A., Wang, Y., Krechmer, J. E., Lambe, A., Majluf, F., Morris, M. A.,
936 Priestley, M., Bannan, T. J., Bryant, D. J., Pereira, K. L., Hamilton, J. F., Rickard, A.
937 R., Newland, M. J., Stark, H., Croteau, P., Jayne, J. T., Worsnop, D. R., Canagaratna,
938 M. R., Wang, L. and Coe, H.: Evaluation of the chemical composition of gas- and
939 particle-phase products of aromatic oxidation, Atmos. Chem. Phys., 20(16), 9783–
940 9803, doi:10.5194/acp-20-9783-2020, 2020.
941 Mellouki, A., Wallington, T. J. and Chen, J.: Atmospheric Chemistry of Oxygenated
942 Volatile Organic Compounds: Impacts on Air Quality and Climate, Chem. Rev.,
943 115(10), 3984–4014, doi:10.1021/cr500549n, 2015.
944 Mohr, C., Lopez-Hilfiker, F. D., Zotter, P., Prévôt, A. S. H., Xu, L., Ng, N. L.,
945 Herndon, S. C., Williams, L. R., Franklin, J. P., Zahniser, M. S., Worsnop, D. R.,
946 Knighton, W. B., Aiken, A. C., Gorkowski, K. J., Dubey, M. K., Allan, J. D. and
947 Thornton, J. A.: Contribution of Nitrated Phenols to Wood Burning Brown Carbon
948 Light Absorption in Detling, United Kingdom during Winter Time, Environ. Sci.
949 Technol., 47(12), 6316–6324, doi:10.1021/es400683v, 2013.
950 Mutzel, A., Poulain, L., Berndt, T., Iinuma, Y., Rodigast, M., Böge, O., Richters, S.,
951 Spindler, G., Sipila¨, M., Jokinen, T., Kulmala, M. and Herrmann, H.: Highly
952 Oxidized Multifunctional Organic Compounds Observed in Tropospheric Particles: A
953 Field and Laboratory Study, Environ. Sci. Technol., 49(13), 7754–7761,
954 doi:10.1021/acs.est.5b00885, 2015.
955 Mutzel, A., Rodigast, M., Iinuma, Y., Böge, O. and Herrmann, H.: Monoterpene SOA
956 - Contribution of first-generation oxidation products to formation and chemical

https://doi.org/10.5194/acp-2020-1187
Preprint. Discussion started: 25 November 2020

composition, Atmos. Environ., 130, 136–144, doi:10.1016/j.atmosenv.2015.10.080, 2016.

Nah, T., Sanchez, J., Boyd, C. M. and Ng, N. L.: Photochemical Aging of α-pinene and β-pinene Secondary Organic Aerosol formed from Nitrate Radical Oxidation, Environ. Sci. Technol., 50(1), 222–231, doi:10.1021/acs.est.5b04594, 2016.

Nannoolal, Y., Rarey, J. and Ramjugernath, D.: Estimation of pure component properties Part 3. Estimation of the vapor pressure of non-electrolyte organic compounds via group contributions and group interactions, Fluid Phase Equilib., 269(1–2), 117–133, doi:10.1016/j.fluid.2008.04.020, 2008.

Ng, N. L., Brown, S. S., Archibald, A. T., Atlas, E., Cohen, R. C., Crowley, J. N., Day, D. A., Donahue, N. M., Fry, J. L., Fuchs, H., Griffin, R. J., Guzman, M. I., Herrmann, H., Hodzic, A., Iinuma, Y., Jimenez, J. L., Kiendler-Scharr, A., Lee, B. H., Luecken, D. J., Mao, J., McLaren, R., Mutzel, A., Osthoff, H. D., Ouyang, B., Picquet-Varrault, B., Platt, U., Pye, H. O. T., Rudich, Y., Schwantes, R. H., Shiraiwa, M., Stutz, J., Thornton, J. A., Tilgner, A., Williams, B. J. and Zaveri, R. A.: Nitrate radicals and biogenic volatile organic compounds: oxidation, mechanisms, and organic aerosol, Atmos. Chem. Phys., 17(3), 2103–2162, doi:10.5194/acp-17-2103-2017, 2017.

Noelscher, A. C., Yanez-Serrano, A. M., Wolff, S., de Araujo, A. C., Lavric, J. V, Kesselmeier, J. and Williams, J.: Unexpected seasonality in quantity and composition of Amazon rainforest air reactivity, Nat. Commun., 7, doi:10.1038/ncomms10383, 2016.

Osthoff, H. D., Roberts, J. M., Ravishankara, A. R., Williams, E. J., Lerner, B. M., Sommariva, R., Bates, T. S., Coffman, D., Quinn, P. K., Dibb, J. E., Stark, H., Burkholder, J. B., Talukdar, R. K., Meagher, J., Fehsenfeld, F. C. and Brown, S. S.: High levels of nitryl chloride in the polluted subtropical marine boundary layer, Nat. Geosci., 1(5), 324–328, doi:10.1038/ngeo177, 2008.

Palm, B. B., Liu, X., Jimenez, J. L. and Thornton, J. A.: Performance of a new coaxial ion-molecule reaction region for low-pressure chemical ionization mass spectrometry with reduced instrument wall interactions, Atmos. Meas. Tech., 12(11), 5829–5844,

https://doi.org/10.5194/acp-2020-1187
Preprint. Discussion started: 25 November 2020


Atmospheric Chemistry and Physics Discussions

987 doi:10.5194/amt-12-5829-2019, 2019.
988 Pankow, J. F. and Asher, W. E.: SIMPOL.1: A simple group contribution method for
989 predicting vapor pressures and enthalpies of vaporization of multifunctional organic
990 compounds, Atmos. Chem. Phys., 8(10), 2773–2796, doi:10.5194/acp-8-2773-2008,
991 2008.
992 Paulot, F., Crounse, J. D., Kjaergaard, H. G., Kroll, J. H., Seinfeld, J. H. and
993 Wennberg, P. O.: Isoprene photooxidation: New insights into the production of acids
994 and organic nitrates, Atmos. Chem. Phys., 9(4), 1479–1501, doi:10.5194/acp-9-1479-
995 2009, 2009.
996 Qi, L., Chen, M., Stefenelli, G., Pospisilova, V., Tong, Y., Bertrand, A., Hueglin, C.,
997 Ge, X., Baltensperger, U., Prévôt, A. S. H. and Slowik, J. G.: Organic aerosol source
998 apportionment in Zurich using an extractive electrospray ionization time-of-flight
999 mass spectrometer (EESI-TOF-MS) – Part 2: Biomass burning influences in winter,
1000 Atmos. Chem. Phys., 19(12), 8037–8062, doi:10.5194/acp-19-8037-2019, 2019.
1001 Reyes-Villegas, E., Bannan, T., Le Breton, M., Mehra, A., Priestley, M., Percival, C.,
1002 Coe, H. and Allan, J. D.: Online Chemical Characterization of Food-Cooking Organic
1003 Aerosols: Implications for Source Apportionment, Environ. Sci. Technol., 52(9),
1004 5308–5318, doi:10.1021/acs.est.7b06278, 2018.
1005 Riva, M., Rantala, P., Krechmer, J. E., Peräkylä, O., Zhang, Y., Heikkinen, L.,
1006 Garmash, O., Yan, C., Kulmala, M., Worsnop, D. and Ehn, M.: Evaluating the
1007 performance of five different chemical ionization techniques for detecting gaseous
1008 oxygenated organic species, Atmos. Meas. Tech., 2018(4), 1–39, doi:10.5194/amt-
1009 2018-407, 2019.
1010 Sander, R. and Crutzen, P. J.: Model study indicating halogen activation and ozone
1011 destruction in polluted air masses transported to the sea, J. Geophys. Res. Atmos.,
1012 101(D4), 9121–9138, doi:10.1029/95JD03793, 1996.
1013 Schneider, J., Weimer, S., Drewnick, F., Borrmann, S., Helas, G., Gwaze, P., Schmid,
1014 O., Andreae, M. O. and Kirchner, U.: Mass spectrometric analysis and aerodynamic
1015 properties of various types of combustion-related aerosol particles, Int. J. Mass
1016 Spectrom., 258(1), 37–49, doi:https://doi.org/10.1016/j.ijms.2006.07.008, 2006.

https://doi.org/10.5194/acp-2020-1187
Preprint. Discussion started: 25 November 2020

1017 Schwantes, R. H., Teng, A. P., Nguyen, T. B., Coggon, M. M., Crounse, J. D., St
1018 Clair, J. M., Zhang, X., Schilling, K. A., Seinfeld, J. H. and Wennberg, P. O.:
1019 Isoprene NO3 Oxidation Products from the RO2 + HO2 Pathway, J. Phys. Chem. A,
1020 119, 10158, 2015.
1021 Schwantes, R. H., Schilling, K. A., McVay, R. C., Lignell, H., Coggon, M. M.,
1022 Zhang, X., Wennberg, P. O. and Seinfeld, J. H.: Formation of highly oxygenated low-
1023 volatility products from cresol oxidation, Atmos. Chem. Phys., 17(5), 3453–3474,
1024 doi:10.5194/acp-17-3453-2017, 2017.
1025 Schwantes, R. H., Emmons, L. K., Orlando, J. J., Barth, M. C., Tyndall, G. S., Hall, S.
1026 R., Ullmann, K., St. Clair, J. M., Blake, D. R., Wisthaler, A. and Paul V. Bui, T.:
1027 Comprehensive isoprene and terpene gas-phase chemistry improves simulated surface
1028 ozone in the southeastern US, Atmos. Chem. Phys., 20(6), 3739–3776,
1029 doi:10.5194/acp-20-3739-2020, 2020.
1030 Shrivastava, M., Andreae, M. O., Artaxo, P., Barbosa, H. M. J., Berg, L. K., Brito, J.,
1031 Ching, J., Easter, R. C., Fan, J., Fast, J. D., Feng, Z., Fuentes, J. D., Glasius, M.,
1032 Goldstein, A. H., Alves, E. G., Gomes, H., Gu, D., Guenther, A., Jathar, S. H., Kim,
1033 S., Liu, Y., Lou, S., Martin, S. T., McNeill, V. F., Medeiros, A., de Sá, S. S., Shilling,
1034 J. E., Springston, S. R., Souza, R. A. F., Thornton, J. A., Isaacman-VanWertz, G.,
1035 Yee, L. D., Ynoue, R., Zaveri, R. A., Zelenyuk, A. and Zhao, C.: Urban pollution
1036 greatly enhances formation of natural aerosols over the Amazon rainforest, Nat.
1037 Commun., 10(1), doi:10.1038/s41467-019-08909-4, 2019.
1038 Simoneit, B. R. T., Schauer, J. J., Nolte, C. G., Oros, D. R., Elias, V. O., Fraser, M.
1039 P., Rogge, W. F. and Cass, G. R.: Levoglucosan, a tracer for cellulose in biomass
1040 burning and atmospheric particles, Atmos. Environ., 33(2), 173–182,
1041 doi:https://doi.org/10.1016/S1352-2310(98)00145-9, 1999.
1042 Stark, H., Yatavelli, R. L. N., Thompson, S. L., Kimmel, J. R., Cubison, M. J.,
1043 Chhabra, P. S., Canagaratna, M. R., Jayne, J. T., Worsnop, D. R. and Jimenez, J. L.:
1044 Methods to extract molecular and bulk chemical information from series of complex
1045 mass spectra with limited mass resolution, Int. J. Mass Spectrom., 389, 26–38,
1046 doi:10.1016/j.ijms.2015.08.011, 2015.

https://doi.org/10.5194/acp-2020-1187
Preprint. Discussion started: 25 November 2020

1047 Stark, H., Yatavelli, R. L. N., Thompson, S. L., Kang, H., Krechmer, J. E., Kimmel, J.
1048 R., Palm, B. B., Hu, W., Hayes, P. L., Day, D. A., Campuzano-Jost, P., Canagaratna,
1049 M. R., Jayne, J. T., Worsnop, D. R. and Jimenez, J. L.: Impact of Thermal
1050 Decomposition on Thermal Desorption Instruments: Advantage of Thermogram
1051 Analysis for Quantifying Volatility Distributions of Organic Species, Environ. Sci.
1052 Technol., 51(15), 8491–8500, doi:10.1021/acs.est.7b00160, 2017.
1053 Stolzenburg, D., Fischer, L., Vogel, A. L., Heinritzi, M., Schervish, M., Simon, M.,
1054 Wagner, A. C., Dada, L., Ahonen, L. R., Amorim, A., Baccarini, A., Bauer, P. S.,
1055 Baumgartner, B., Bergen, A., Bianchi, F., Breitenlechner, M., Brilke, S., Buenrostro
1056 Mazon, S., Chen, D., Dias, A., Draper, D. C., Duplissy, J., El Haddad, I.,
1057 Finkenzeller, H., Frege, C., Fuchs, C., Garmash, O., Gordon, H., He, X., Helm, J.,
1058 Hofbauer, V., Hoyle, C. R., Kim, C., Kirkby, J., Kontkanen, J., Kürten, A.,
1059 Lampilahti, J., Lawler, M., Lehtipalo, K., Leiminger, M., Mai, H., Mathot, S.,
1060 Mentler, B., Molteni, U., Nie, W., Nieminen, T., Nowak, J. B., Ojdanic, A., Onnela,
1061 A., Passananti, M., Petäjä, T., Quéléver, L. L. J., Rissanen, M. P., Sarnela, N.,
1062 Schallhart, S., Tauber, C., Tomé, A., Wagner, R., Wang, M., Weitz, L., Wimmer, D.,
1063 Xiao, M., Yan, C., Ye, P., Zha, Q., Baltensperger, U., Curtius, J., Dommen, J., Flagan,
1064 R. C., Kulmala, M., Smith, J. N., Worsnop, D. R., Hansel, A., Donahue, N. M. and
1065 Winkler, P. M.: Rapid growth of organic aerosol nanoparticles over a wide
1066 tropospheric temperature range, Proc. Natl. Acad. Sci., 115(37), 201807604,
1067 doi:10.1073/pnas.1807604115, 2018.
1068 Surratt, J. D., Murphy, S. M., Kroll, J. H., Ng, N. L., Hildebrandt, L., Sorooshian, A.,
1069 Szmigielski, R., Vermeylen, R., Maenhaut, W., Claeys, M., Flagan, R. C. and
1070 Seinfeld, J. H.: Chemical Composition of Secondary Organic Aerosol Formed from
1071 the Photooxidation of Isoprene, J. Phys. Chem. A, 110(31), 9665–9690,
1072 doi:10.1021/jp061734m, 2006.
1073 Surratt, J. D., Kroll, J. H., Kleindienst, T. E., Edney, E. O., Claeys, M., Sorooshian,
1074 A., Ng, N. L., Offenberg, J. H., Lewandowski, M., Jaoui, M., Flagan, R. C. and
1075 Seinfeld, J. H.: Evidence for Organosulfates in Secondary Organic Aerosol, Environ.
1076 Sci. Technol., 41(2), 517–527, doi:10.1021/es062081q, 2007.

https://doi.org/10.5194/acp-2020-1187
Preprint. Discussion started: 25 November 2020

1077 Surratt, J. D., Chan, A. W. H., Eddingsaas, N. C., Chan, M., Loza, C. L., Kwan, A. J.,
1078 Hersey, S. P., Flagan, R. C., Wennberg, P. O. and Seinfeld, J. H.: Reactive
1079 intermediates revealed in secondary organic aerosol formation from isoprene, Proc.
1080 Natl. Acad. Sci., 107(15), 6640–6645, doi:10.1073/pnas.0911114107, 2010.
1081 Thornton, J. A., Mohr, C., Schobesberger, S., D'Ambro, E. L., Lee, B. H. and Lopez-
1082 Hilfiker, F. D.: Evaluating Organic Aerosol Sources and Evolution with a Combined
1083 Molecular Composition and Volatility Framework Using the Filter Inlet for Gases and
1084 Aerosols (FIGAERO), Acc. Chem. Res., 53(8), 1415–1426,
1085 doi:10.1021/acs.accounts.0c00259, 2020.
1086 Volkamer, R., Jimenez, J. L., San Martini, F., Dzepina, K., Zhang, Q., Salcedo, D.,
1087 Molina, L. T., Worsnop, D. R. and Molina, M. J.: Secondary organic aerosol
1088 formation from anthropogenic air pollution: Rapid and higher than expected,
1089 Geophys. Res. Lett., 33(17), doi:10.1029/2006GL026899, 2006.
1090 Wang, B. and LinHo: Rainy Season of the Asian–Pacific Summer Monsoon*, J.
1091 Clim., 15(4), 386–398, doi:10.1175/1520-0442(2002)015<0386:RSOTAP>2.0.CO;2,
1092 2002.
1093 Wang, H., Gao, Y., Wang, S., Wu, X., Liu, Y., Li, X., Huang, D., Lou, S., Wu, Z.,
1094 Guo, S., Jing, S., Li, Y., Huang, C., Tyndall, G. S., Orlando, J. J. and Zhang, X.:
1095 Atmospheric Processing of Nitrophenols and Nitrocresols from Biomass Burning
1096 Emissions, J. Geophys. Res. Atmos., 0–3, doi:10.1029/2020JD033401, 2020a.
1097 Wang, M., Chen, D., Xiao, M., Ye, Q., Stolzenburg, D., Hofbauer, V., Ye, P., Vogel,
1098 A. L., Mauldin, R. L., Amorim, A., Baccarini, A., Baumgartner, B., Brilke, S., Dada,
1099 L., Dias, A., Duplissy, J., Finkenzeller, H., Garmash, O., He, X.-C., Hoyle, C. R.,
1100 Kim, C., Kvashnin, A., Lehtipalo, K., Fischer, L., Molteni, U., Petäjä, T., Pospisilova,
1101 V., Quéléver, L. L. J., Rissanen, M., Simon, M., Tauber, C., Tomé, A., Wagner, A. C.,
1102 Weitz, L., Volkamer, R., Winkler, P. M., Kirkby, J., Worsnop, D. R., Kulmala, M.,
1103 Baltensperger, U., Dommen, J., El-Haddad, I. and Donahue, N. M.: Photo-oxidation
1104 of Aromatic Hydrocarbons Produces Low-Volatility Organic Compounds, Environ.
1105 Sci. Technol., 54(13), 7911–7921, doi:10.1021/acs.est.0c02100, 2020b.
1106 Wang, T., Tham, Y. J., Xue, L., Li, Q., Zha, Q., Wang, Z., Poon, S. C. N., Dube, W.

https://doi.org/10.5194/acp-2020-1187
Preprint. Discussion started: 25 November 2020

1107 P., Blake, D. R., Louie, P. K. K., Luk, C. W. Y., Tsui, W., Brown, S. S., Osthoff, H.
1108 D., Roberts, J. M., Ravishankara, A. R., Williams, E. J., Lerner, B. M., Sommariva,
1109 R., Bates, T. S., Coffman, D., Quinn, P. K., Dibb, J. E., Stark, H., Burkholder, J. B.,
1110 Talukdar, R. K., Meagher, J., Fehsenfeld, F. C. and Brown, S. S.: Observations of
1111 nitryl chloride and modeling its source and effect on ozone in the planetary boundary
1112 layer of southern China, J. Geophys. Res., 121(5), 2476–2489,
1113 doi:10.1002/2015JD024556, 2016.
1114 Wang, X., Jacob, D. J., Eastham, S. D., Sulprizio, M. P., Zhu, L., Chen, Q.,
1115 Alexander, B., Sherwen, T., Evans, M. J., Lee, B. H., Haskins, J. D., Lopez-Hilfiker,
1116 F. D., Thornton, J. A., Huey, G. L. and Liao, H.: The role of chlorine in global
1117 tropospheric chemistry, Atmos. Chem. Phys., 19(6), 3981–4003, doi:10.5194/acp-19-
1118 3981-2019, 2019.
1119 Wang, Z., Yuan, B., Ye, C., Roberts, J., Wisthaler, A., Lin, Y., Li, T., Wu, C., Peng,
1120 Y., Wang, C., Wang, S., Yang, S., Wang, B., Qi, J., Wang, C., Song, W., Hu, W.,
1121 Wang, X., Xu, W., Ma, N., Kuang, Y., Tao, J., Zhang, Z., Su, H., Cheng, Y., Wang,
1122 X. and Shao, M.: High Concentrations of Atmospheric Isocyanic Acid (HNCO)
1123 Produced from Secondary Sources in China, Environ. Sci. Technol.,
1124 doi:10.1021/acs.est.0c02843, 2020c.
1125 Wennberg, P. O., Bates, K. H., Crounse, J. D., Dodson, L. G., McVay, R. C., Mertens,
1126 L. A., Nguyen, T. B., Praske, E., Schwantes, R. H., Smarte, M. D., St Clair, J. M.,
1127 Teng, A. P., Zhang, X. and Seinfeld, J. H.: Gas-Phase Reactions of Isoprene and Its
1128 Major Oxidation Products, Chem. Rev., 118(7), 3337–3390,
1129 doi:10.1021/acs.chemrev.7b00439, 2018.
1130 Wu, C., Wang, C., Wang, S., Wang, W., Yuan, B., Qi, J., Wang, B., Wang, H., Wang,
1131 C., Song, W., Wang, X., Hu, W., Lou, S., Ye, C., Peng, Y., Wang, Z., Huangfu, Y.,
1132 Xie, Y., Zhu, M., Zheng, J., Wang, X., Jiang, B., Zhang, Z. and Shao, M.: Important
1133 contributions of oxygenated compounds to emissions and chemistry of VOCs in urban
1134 air, Atmos. Chem. Phys. Discuss., 2020, 1–37, doi:10.5194/acp-2020-152, 2020.
1135 Xiong, F., McAvey, K. M., Pratt, K. A., Groff, C. J., Hostetler, M. A., Lipton, M. A.,
1136 Starn, T. K., Seeley, J. V, Bertman, S. B. and Teng, A. P.: Observation of Isoprene

https://doi.org/10.5194/acp-2020-1187
Preprint. Discussion started: 25 November 2020

Hydroxynitrates in the Southeastern United States and Implications for the Fate of NOx, Atmos. Chem. Phys., 15, 11257, 2015.

Xue, L., Gu, R., Wang, T., Wang, X., Saunders, S., Blake, D., Louie, P. K. K., Luk, C. W. Y., Simpson, I., Xu, Z., Wang, Z., Gao, Y., Lee, S., Mellouki, A. and Wang, W.: Oxidative capacity and radical chemistry in the polluted atmosphere of Hong Kong and Pearl River Delta region: analysis of a severe photochemical smog episode, Atmos. Chem. Phys., 16(15), 9891–9903, doi:10.5194/acp-16-9891-2016, 2016.

Yang, Y., Shao, M., Wang, X., Nölscher, A. C., Kessel, S., Guenther, A. and Williams, J.: Towards a quantitative understanding of total OH reactivity: A review, Atmos. Environ., 134(2), 147–161, doi:10.1016/j.atmosenv.2016.03.010, 2016.

Yang, Y., Shao, M., Keßel, S., Li, Y., Lu, K., Lu, S., Williams, J., Zhang, Y., Zeng, L., Nölscher, A. C., Wu, Y., Wang, X. and Zheng, J.: How the OH reactivity affects the ozone production efficiency: case studies in Beijing and Heshan, China, Atmos. Chem. Phys., 17(11), 7127–7142, doi:10.5194/acp-17-7127-2017, 2017.

Yasmeen, F., Szmigielski, R., Vermeylen, R., Gomez-Gonzalez, Y., Surratt, J. D., Chan, A. W. H., Seinfeld, J. H., Maenhaut, W. and Claeys, M.: Mass spectrometric characterization of isomeric terpenoic acids from the oxidation of alpha-pinene, beta-pinene, d-limonene, and Delta(3)-carene in fine forest aerosol, J. MASS Spectrom., 46(4), 425–442, doi:10.1002/jms.1911, 2011.

Yihui, D. and Chan, J. C. L.: The East Asian summer monsoon: an overview, Meteorol. Atmos. Phys., 89(1), 117–142, doi:10.1007/s00703-005-0125-z, 2005.

Yuan, B., Veres, P. R., Warneke, C., Roberts, J. M., Gilman, J. B., Koss, A., Edwards, P. M., Graus, M., Kuster, W. C., Li, S. M., Wild, R. J., Brown, S. S., Dubé, W. P., Lerner, B. M., Williams, E. J., Johnson, J. E., Quinn, P. K., Bates, T. S., Lefer, B., Hayes, P. L., Jimenez, J. L., Weber, R. J., Zamora, R., Ervens, B., Millet, D. B., Rappenglück, B. and De Gouw, J. A.: Investigation of secondary formation of formic acid: Urban environment vs. oil and gas producing region, Atmos. Chem. Phys., 15(4), 1975–1993, doi:10.5194/acp-15-1975-2015, 2015.

Yuan, B., Liggio, J., Wentzell, J., Li, S. M., Stark, H., Roberts, J. M., Gilman, J., Lerner, B., Warneke, C., Li, R., Leithead, A., Osthoff, H. D., Wild, R., Brown, S. S.

https://doi.org/10.5194/acp-2020-1187
Preprint. Discussion started: 25 November 2020

Atmospheric Chemistry and Physics Discussions

1167 and De Gouw, J. A.: Secondary formation of nitrated phenols: Insights from
1168 observations during the Uintah Basin Winter Ozone Study (UBWOS) 2014, Atmos.
1169 Chem. Phys., 16(4), 2139–2153, doi:10.5194/acp-16-2139-2016, 2016.
1170 Yuan, B., Koss, A. R., Warneke, C., Coggon, M., Sekimoto, K. and De Gouw, J. A.:
1171 Proton-Transfer-Reaction Mass Spectrometry: Applications in Atmospheric Sciences,
1172 Chem. Rev., 117(21), 13187–13229, doi:10.1021/acs.chemrev.7b00325, 2017.
1173 Zhang, Q., Yuan, B., Shao, M., Wang, X., Lu, S., Lu, K., Wang, M., Chen, L., Chang,
1174 C.-C. and Liu, S. C.: Variations of ground-level O3 and its precursors in Beijing in
1175 summertime between 2005 and 2011, Atmos. Chem. Phys., 14(12), 6089–6101,
1176 doi:10.5194/acp-14-6089-2014, 2014.
1177 Zhao, R.: The Recent Development and Application of Chemical Ionization Mass
1178 Spectrometry in Atmospheric Chemistry., 2018.
1179 Zhao, Y., Nguyen, N. T., Presto, A. A., Hennigan, C. J., May, A. A. and Robinson, A.
1180 L.: Intermediate Volatility Organic Compound Emissions from On-Road Gasoline
1181 Vehicles and Small Off-Road Gasoline Engines, Environ. Sci. Technol., 50(8), 4554–
1182 4563, doi:10.1021/acs.est.5b06247, 2016.
1183 Zhou, Y., Huang, X. H., Bian, Q., Griffith, S. M., Louie, P. K. K. and Yu, J. Z.:
1184 Sources and atmospheric processes impacting oxalate at a suburban coastal site in
1185 Hong Kong: Insights inferred from 1 year hourly measurements, J. Geophys. Res.
1186 Atmos., 120(18), 9772–9788, doi:10.1002/2015JD023531, 2015.
1187

https://doi.org/10.5194/acp-2020-1187
Preprint. Discussion started: 25 November 2020

Atmospheric Chemistry and Physics Discussions

1188 **Table 1.** The detected ions discussed in the text.

Ion formula	m/z	Assigned compounds	Possible formation pathways	References
$C_6H_{10}O_5I$	288.96	Levoglucosan, mannosan and galactosan	Biomass burning or cooking emissions	(Gaston et al., 2016; Reyes-Villegas et al., 2018)
$C_6H_{12}O_5I^-$	290.97	Fucose	Biomass burning emissions	(Qi et al., 2019)
$C_6H_5NO_3I^-$	265.93	Nitro-phenols	Direct emissions, oxidation of aromatics in the presence of NOx	(Gaston et al., 2016; Yuan et al., 2016)
$C_6H_5NO_4I^-$	281.93	Nitro-benzenediols	Direct emissions, oxidation of aromatics in the presence of NOx	(Gaston et al., 2016; Yuan et al., 2016)
$C_6H_4N_2O_5I^-$	310.92	Dinitro-phenols	Direct emissions, oxidation of aromatics in the presence of NOx	(Gaston et al., 2016; Yuan et al., 2016)
$C_7H_7NO_3I^-$	279.95	Methyl nitro-phenols	Direct emissions, oxidation of aromatics in the presence of NOx	(Gaston et al., 2016; Yuan et al., 2016)
$C_7H_7NO_4I^-$	295.94	Methyl nitro-benzenediols	Direct emissions, oxidation of aromatics in the presence of NOx	(Gaston et al., 2016; Yuan et al., 2016)
$C_7H_6O_4I^-$	280.93	Dihydroxy methyl benzoquinone	Aromatics + OH	(Schwantes et al., 2017; Wang et al., 2020b)
$C_7H_8O_4I^-$	282.95	Tetrahydroxy toluene	Aromatics + OH	(Schwantes et al., 2017; Wang et al., 2020b)
$C_7H_8O_5I^-$	298.94	Pentahydroxy toluene, fragments of C9 aromatics	Aromatics + OH	(Mehra et al., 2020; Schwantes et al., 2017)

https://doi.org/10.5194/acp-2020-1187
Preprint. Discussion started: 25 November 2020

Atmospheric Chemistry and Physics Discussions

$CH_2O_2I^-$	172.91	Formic acid	Oxidation of VOCs	(Lee et al., 2014; Yuan et al., 2015)
$C_2H_4O_2I^-$	186.93	Acetic acid	Oxidation of VOCs	(Lee et al., 2014; Mattila et al., 2018)
$C_5H_{10}O_2I^-$	228.97	Pentanoic acid	Traffic emissions, secondary formation	(Mattila et al., 2018)
$C_2H_4O_3I^-$	202.92	Glycolic acid	Oxidation of VOCs	(Lee et al., 2014; Lim et al., 2005)
$C_3H_4O_3I^-$	214.92	Pyruvic acid	Photolysis of methylglyoxal, BVOCs+OH, photo-oxidation of aromatics in the presence of NO_X	(Eger et al., 2020; Mattila et al., 2018)
$C_2H_2O_4I^-$	216.90	Oxalic acid	Aqueous-phase photooxidation of glyoxal, photo-oxidation of VOCs	(Carlton et al., 2007; Lee et al., 2014; Zhou et al., 2015)
$C_3H_4O_4I^-$	230.92	Malonic acid, hydroxypyruvic acid	Oxidation of VOCs	(Kawamura and Bikkina, 2016; Lee et al., 2014)
$C_4H_4O_4I^-$	242.92	Maleic acid, fumaric acid	Oxidation of aromatics	(Brege et al., 2018; Kawamura et al., 1996)
$C_5H_6O_4I^-$	256.93	Unsaturated dicarboxylic acid	Oxidation of aromatics	(Brege et al., 2018; Kawamura et al., 1996)
$C_5H_8O_4I^-$	258.95		Photo-oxidation of VOCs	(Berndt et al., 2019; Kawamura and Bikkina, 2016)
$C_6H_{10}O_4I^-$	272.96		Photo-oxidation of VOCs	(Berndt et al., 2019; Kawamura and Bikkina, 2016)

https://doi.org/10.5194/acp-2020-1187
Preprint. Discussion started: 25 November 2020

$C_4H_8O_4I^-$	246.95	2-methylglyceric acid	Isoprene SOA component under high NOx conditions	(Surratt et al., 2006, 2010)
$C_5H_9NO_4I^-$	273.96	IHN (isoprene hydroxy nitrates)	1st-genetration organic nitrates from reaction: isoprene+OH+NOx, isoprene+NO_3	(Jacobs et al., 2014; Xiong et al., 2015)
$C_4H_7NO_5I^-$	275.94	MVKN/ MACRN	2nd-genetration organic nitrates from oxidation of IHN in the presence of NOx	(Fisher et al., 2016; Paulot et al., 2009)
$C_5H_9NO_5I^-$	289.95	C5 nitrooxy hydroperoxide, C5 nitrooxy hydroxyepoxide, C5 dihydroxy nitrate	isoprene+NO_3, isoprene+OH+NOx	(Ng et al., 2017; Schwantes et al., 2015; Wennberg et al., 2018)
$C_8H_{12}O_4I^-$	298.98	Dicarboxylic and oxocarboxylic acids like norpinic acid, terpenylic acid	Monoterpenes+OH, monoterpenes O_3	(Fang et al., 2017; Mutzel et al., 2016; Yasmeen et al., 2011)
$C_9H_{14}O_4I^-$	312.99	Dicarboxylic and oxocarboxylic acids like pinic acid, homoterpenylic acid, caric acid	Monoterpenes+OH, monoterpenes O_3	(Fang et al., 2017; Mutzel et al., 2016; Yasmeen et al., 2011)
$C_{10}H_{16}O_3I^-$	311.02	Oxocarboxylic acids like	Monoterpenes+OH, monoterpenes O_3	(Fang et al., 2017; Glasius et al.,

https://doi.org/10.5194/acp-2020-1187
Preprint. Discussion started: 25 November 2020

		pinonic acid, caronic acid		2000; Yasmeen et al., 2011)
$C_8H_{13}NO_6I^-$	345.98	Organic nitrates from monoterpenes	Monoterpenes+OH+NO_X, monoterpenes +NO_3	(Lee et al., 2016; Nah et al., 2016)
$C_8H_{11}NO_7I^-$	359.96	Organic nitrates from monoterpenes	Monoterpenes+OH+NO_X, monoterpenes O_3+NO_3	(Carslaw, 2013; Lee et al., 2016)
$C_{10}H_{15}NO_6I^-$	372.00	Organic nitrates from monoterpenes, peroxyacetyl nitrate from pinonaldehyde	Monoterpenes+OH+NO_X, monoterpenes O_3+NO_3	(Boyd et al., 2015; Massoli et al., 2018; Schwantes et al., 2020)
HSO_4^-	96.96	Sulfuric acid	Oxidation of SO_2 etc.	(Le Breton et al., 2018b)
SO_3I^-	206.86	Sulfur trioxide, Fragment of organosulfates	Oxidation of SO_2, decomposition of organosulfates	(Surratt et al., 2007)
$C_2H_3SO_6^-$	154.96	Glycolic acid sulfate	Aqueous reaction of glycolic acid and sulfuric acid	(Galloway et al., 2009; Huang et al., 2018)
$CH_3SO_3^-$	94.98	Methanesulfonic acid	Oxidation of dimethyl sulfide	(Chen and Finlayson-Pitts, 2017; Gondwe et al., 2003)
$N_2O_5I^-$	234.89	Dinitrogen pentoxide	NO_3 + NO_2 + M	(Le Breton et al., 2018a; Wang et al., 2016)
$ClNO_2I^-$	207.87	Nitryl chloride	N_2O_5 (g) + Cl^- (aq)	(Le Breton et al., 2018a; Wang et al., 2016)

https://doi.org/10.5194/acp-2020-1187
Preprint. Discussion started: 25 November 2020

Atmospheric Chemistry and Physics Discussions

$ClNO_3I^-$	223.86	Chlorine nitrate	$ClO + NO_2 + M$	(Liu et al., 2017; Sander and Crutzen, 1996)
Cl_2I^-	196.84	Chlorine	Heterogeneous reactions of Cl^- and reactive chlorine like HOCl, $ClNO_2$ etc.	(Le Breton et al., 2018a; Liu et al., 2017; Wang et al., 2019)
HNO_3I^-	189.90	Nitric acid	NO_X + OH, hydrolysis of organic nitrates and N_2O_5	(Fisher et al., 2016; Wang et al., 2016)

1189

https://doi.org/10.5194/acp-2020-1187
Preprint. Discussion started: 25 November 2020

Atmospheric Chemistry and Physics Discussions

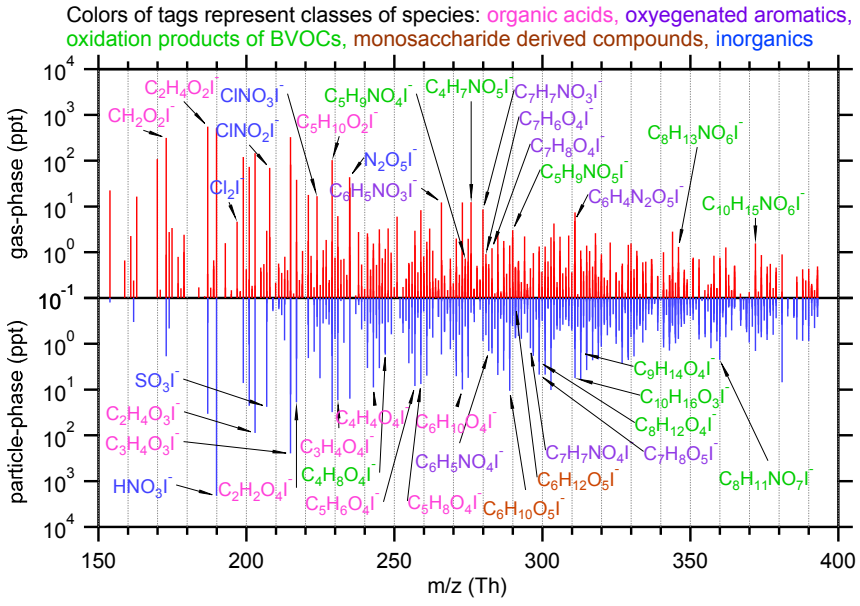

Figure 1. Mass spectra of iodide charged ion within m/z 150~ 400 Th in gas-phase (red) and particle-phase (blue), respectively. Humidity correction was not applied when calculating the averaged concentrations in mass spectra.

https://doi.org/10.5194/acp-2020-1187
Preprint. Discussion started: 25 November 2020

Atmospheric Chemistry and Physics Discussions

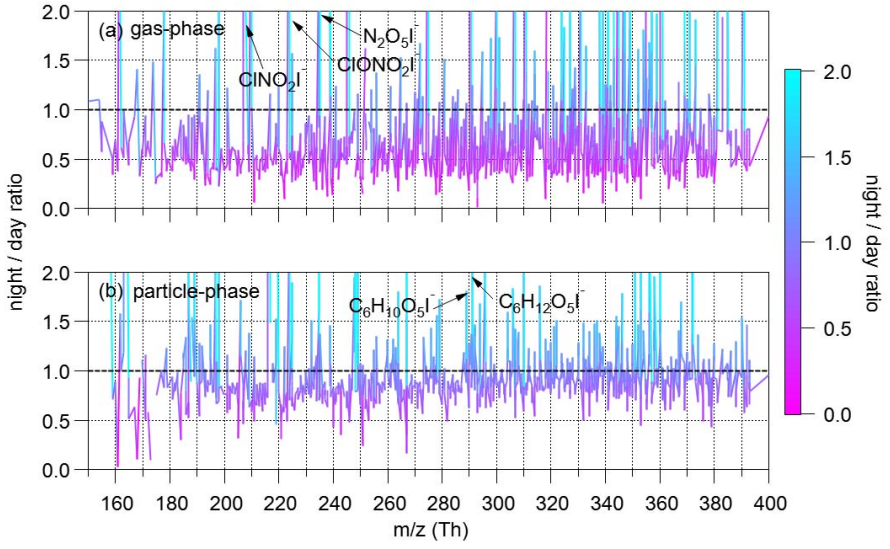

Figure 2. The ratios of concentrations at night (10 pm ~ 6 am) to concentrations during the day (10 am ~ 6 pm) for ions ranging from 150 to 500 Th in gas-phase (a) and particle-phase (b). The range of y-axis is set between 0 and 2 for clarity, although the ratios of some compounds are larger than 2.

https://doi.org/10.5194/acp-2020-1187
Preprint. Discussion started: 25 November 2020

Atmospheric Chemistry and Physics Discussions

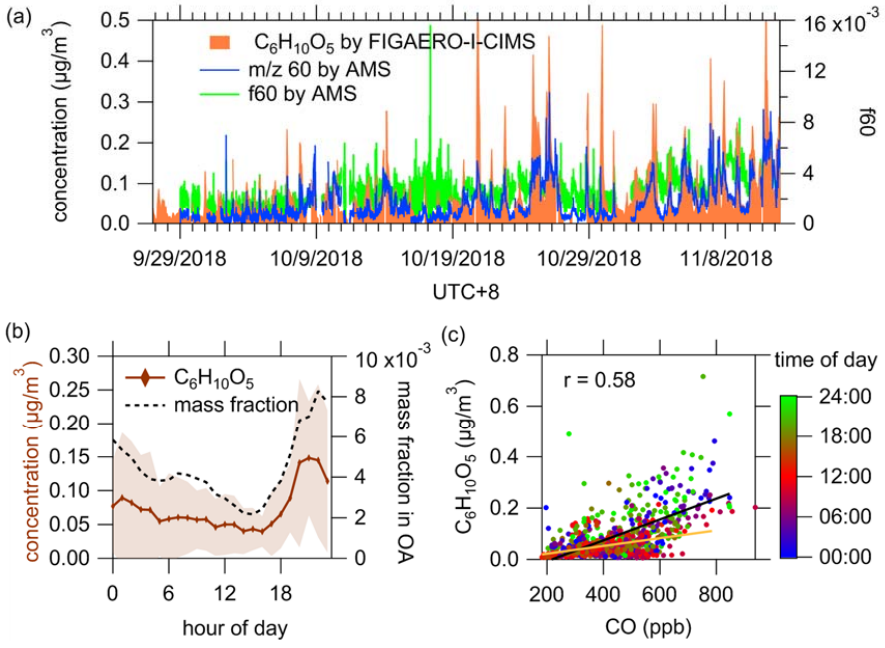

1199

1200 **Figure 3.** (a) Time series of particulate $C_6H_{10}O_5$ measured by FIGAERO-I-CIMS, m/z
1201 60 fragment and f60 measured by AMS. Background f60=0.3% and background m/z
1202 60=0.3%×OA were subtracted from f60 and m/z 60 (Cubison et al., 2011; Hu et al.,
1203 2016). (b) Diurnal variations of particulate $C_6H_{10}O_5$ and its mass fraction in OA. (c)
1204 Correlation between CO and particulate $C_6H_{10}O_5$. The orange and black lines indicate
1205 the ratios during daytime (10 am ~ 6 pm) and nighttime (10 pm ~ 6 am), which are 1.5
1206 $\times 10^{-4}$ and 4.1×10^{-4} ($\mu g \cdot m^{-3}$/ppb), respectively.

https://doi.org/10.5194/acp-2020-1187
Preprint. Discussion started: 25 November 2020

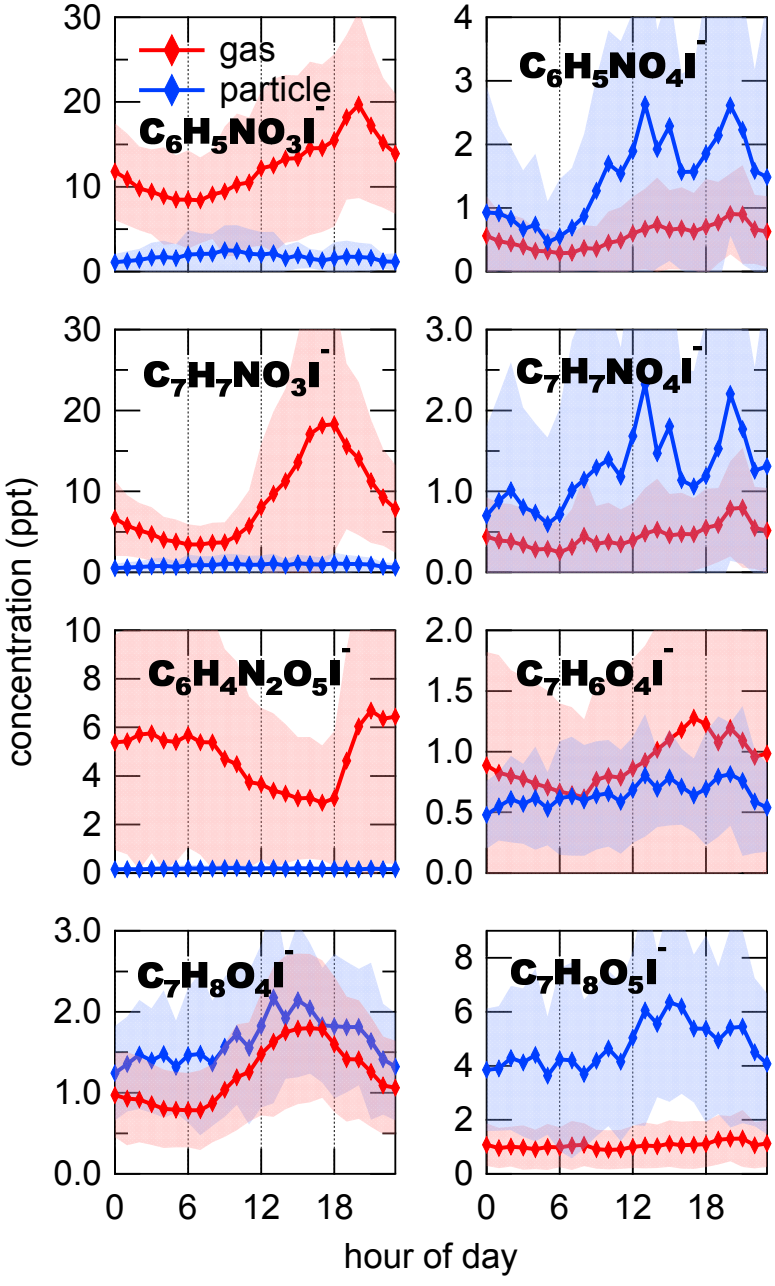

Figure 4. Diurnal variations of oxidized aromatics in both phases. The shaded area indicates standard deviations.

https://doi.org/10.5194/acp-2020-1187
Preprint. Discussion started: 25 November 2020

Atmospheric Chemistry and Physics Discussions

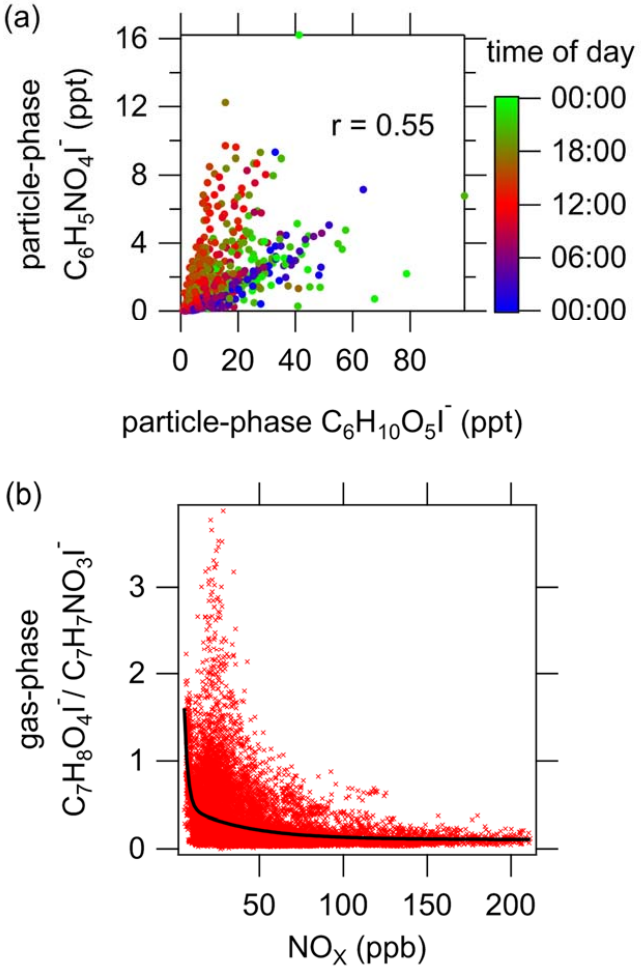

1210

1211 **Figure 5.** (a) Correlation between particle-phase $C_6H_5NO_4I^-$ and $C_6H_{10}O_5I^-$. The
1212 data points are color-coded using the time of the day. (b) Relative concentration of
1213 $C_7H_8O_4I^-$ and $C_7H_7NO_3I^-$ in the gas phase as a function of NOx concentration. The
1214 black line is the fitted curve using a double exponential function.

https://doi.org/10.5194/acp-2020-1187
Preprint. Discussion started: 25 November 2020

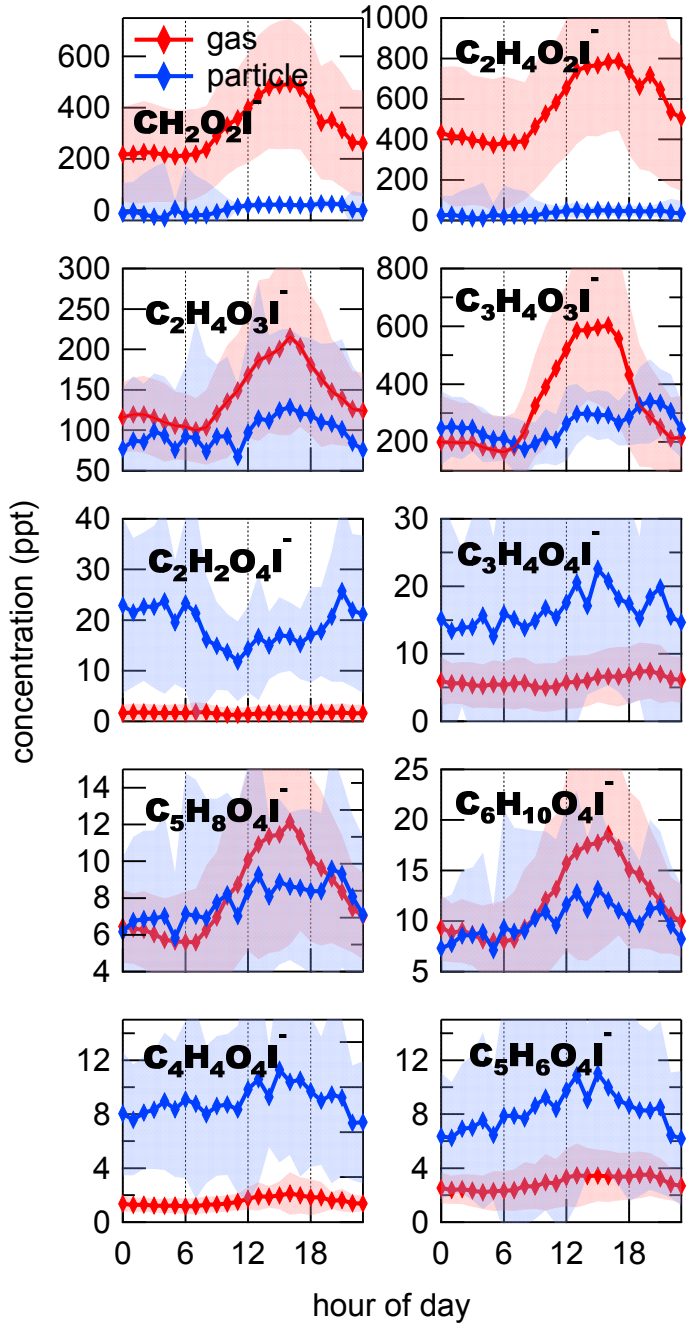

Figure 6. Diurnal variations of organic acids in the gas phase (red) and particle phase (blue). The shaded area indicates standard deviations.

https://doi.org/10.5194/acp-2020-1187
Preprint. Discussion started: 25 November 2020

Atmospheric Chemistry and Physics Discussions

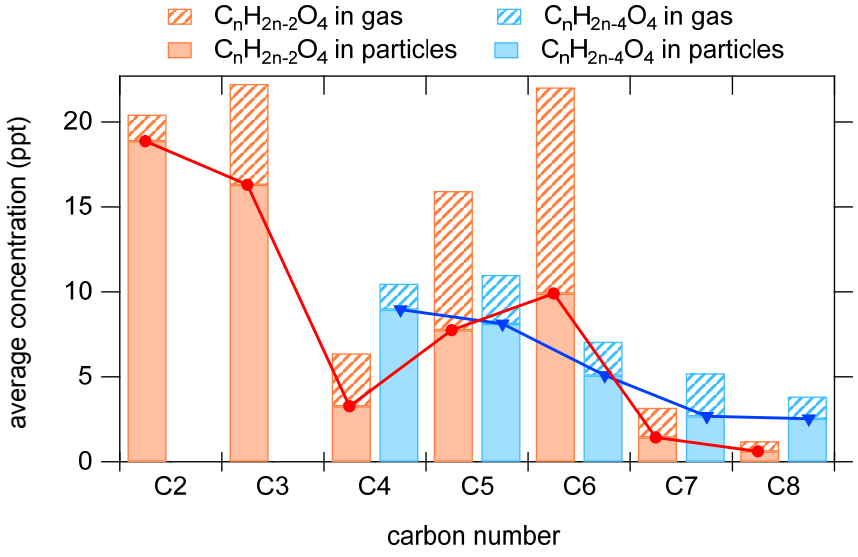

1218

1219 **Figure 7.** Average concentrations of compounds with the formulas of $C_nH_{2n-2}O_4$

1220 and $C_nH_{2n-4}O_4$.

https://doi.org/10.5194/acp-2020-1187
Preprint. Discussion started: 25 November 2020

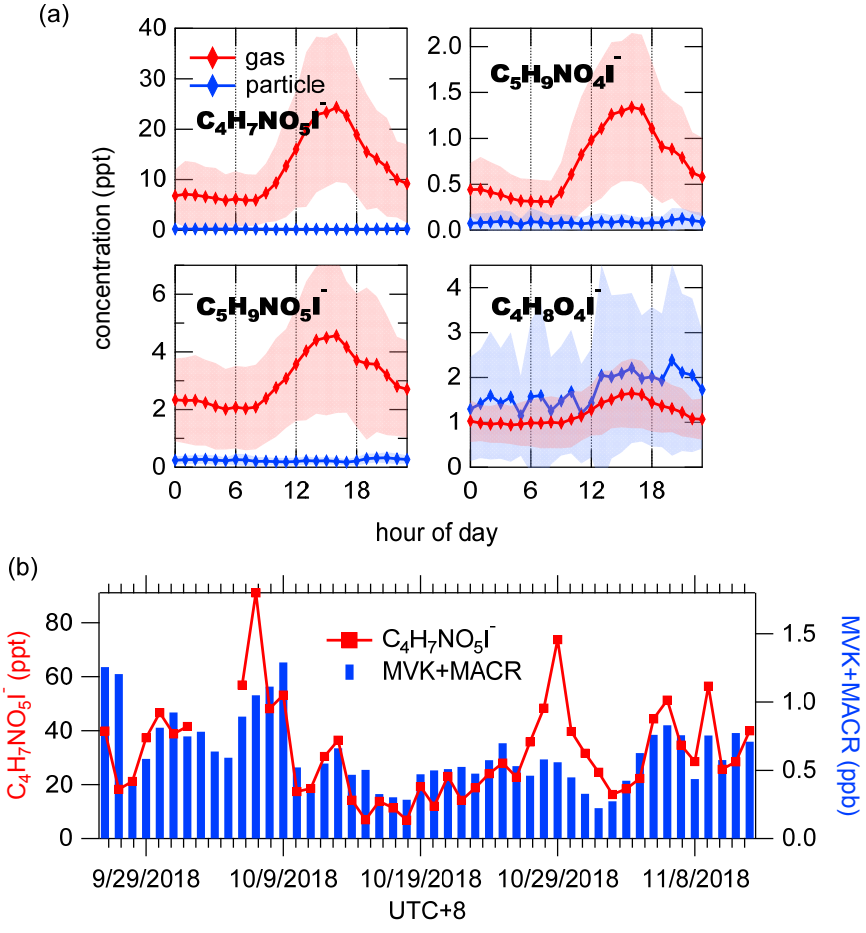

Figure 8. (a) Diurnal variations of isoprene oxidation products in the gas phase (red) and particle phase (blue). The shaded area indicates standard deviations. (b) Time series of daily maximum concentrations of gaseous $C_4H_7NO_5I^-$ and MVK+MACR ($C_4H_6OH^+$, m/z 71.05) measured by PTR-ToF-MS.

https://doi.org/10.5194/acp-2020-1187
Preprint. Discussion started: 25 November 2020

Atmospheric Chemistry and Physics Discussions

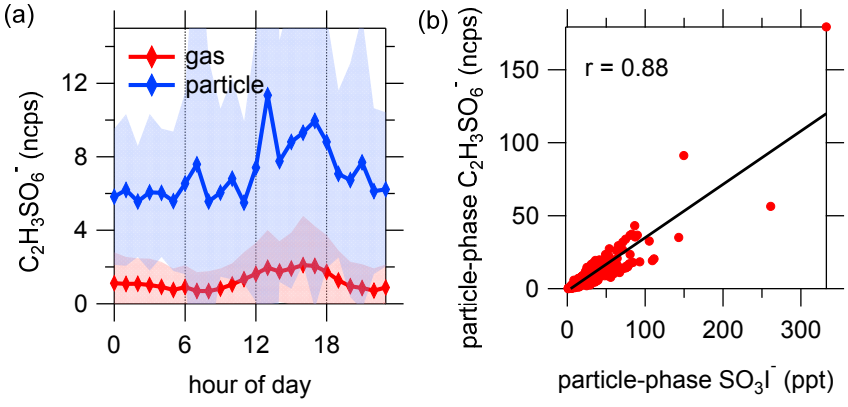

1226

1227 **Figure 9.** (a) Diurnal variation of $C_2H_3SO_6^-$. The shaded areas indicate standard

1228 deviations. (b) Correlation between particle-phase $C_2H_3SO_6^-$ and SO_3I^-.

https://doi.org/10.5194/acp-2020-1187
Preprint. Discussion started: 25 November 2020

Atmospheric Chemistry and Physics Discussions

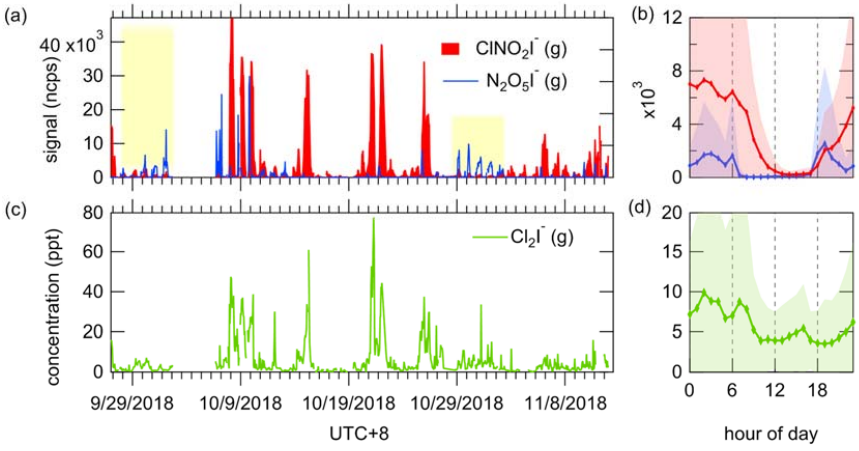

Figure 10. Time series and diurnal variations of N_2O_5 and $ClNO_2$ (a, b) and Cl_2 (c, d). The humidity dependence of the sensitivity of chlorine was experimentally determined and thus humidity-correction was applied to chlorine. The tinted background indicates the days with high concentrations of N_2O_5 but low concentrations of $ClNO_2$. The shaded areas indicate standard deviations.

https://doi.org/10.5194/acp-2020-1187
Preprint. Discussion started: 25 November 2020

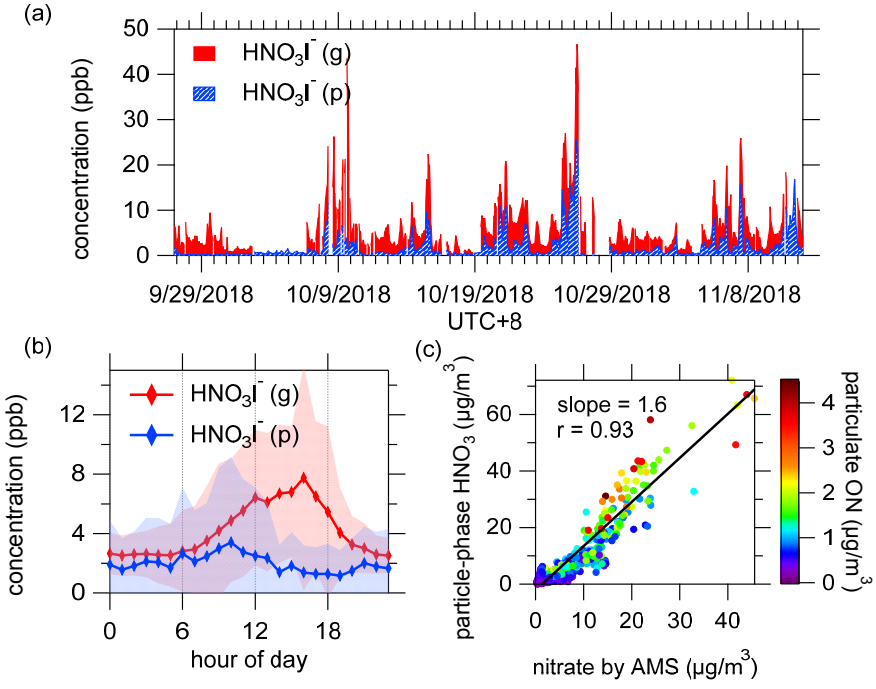

Figure 11. (a) Time series of humidity-corrected HNO_3I^- in both phases. (b) Diurnal variation of humidity-corrected HNO_3I^-. The shaded areas indicate standard deviations. (c) Comparison of particle-phase HNO_3I^- and nitrate measured by AMS. The color scale denotes particulate organic nitrates measured by FIGAERO-I-CIMS. The concentration of gaseous HNO_3I^- shown here only included the last 5-minute of every gas-phase working mode, as high level of HNO_3 came out of aerosol which then passed through the CIMS in a short time during particle analysis and a substantial amount would subsequently accumulate on the inner surfaces, leading to a persistent carried over signal that was long enough to disturb the next gas measurement cycle (Palm et al., 2019).

https://doi.org/10.5194/acp-2020-1187
Preprint. Discussion started: 25 November 2020

Atmospheric Chemistry and Physics Discussions

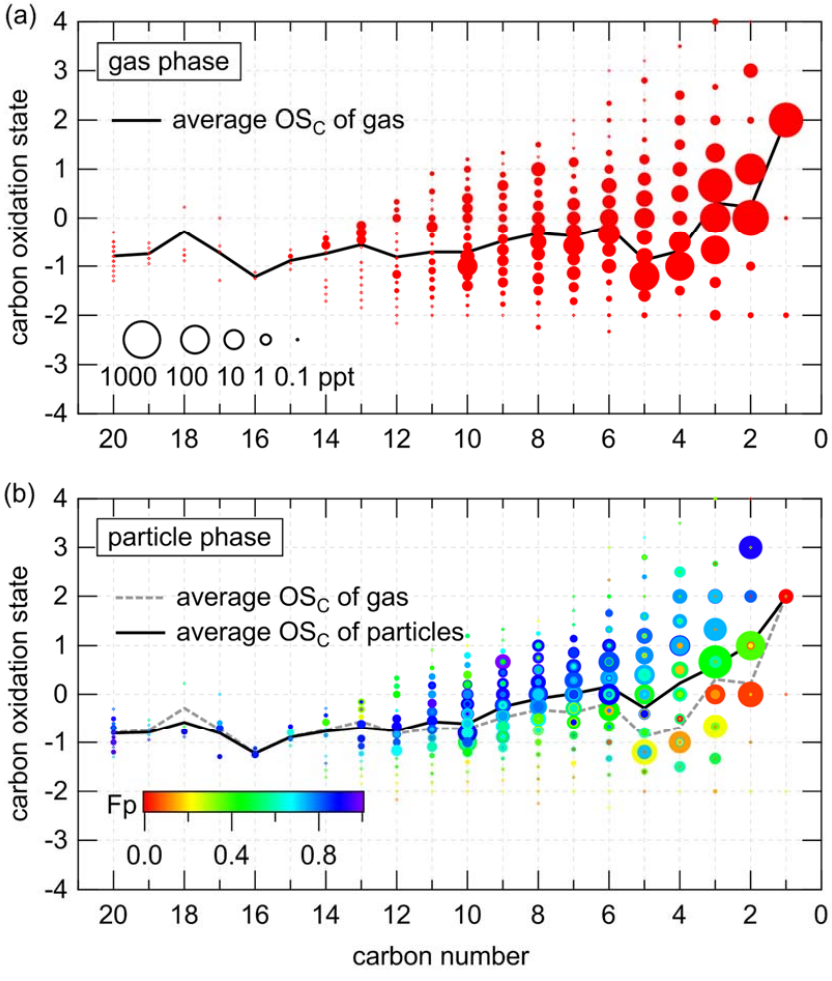

Figure 12. $\overline{OS_C} - n_C$ spaces for $C_xH_yO_z$ and $C_xH_yN_{1,2}O_z$ compounds in gas-phase (a) and particle-phase (b). The diameters of circles are proportional to the logarithmic average concentrations. The black lines are the average $\overline{OS_C}$ of each carbon number for compounds in gas-phase and particle-phase, respectively. The compounds in Fig. (b) are color-coded by their fractions in particles.

https://doi.org/10.5194/acp-2020-1187
Preprint. Discussion started: 25 November 2020

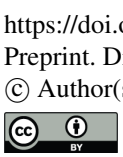

Atmospheric Chemistry and Physics Discussions

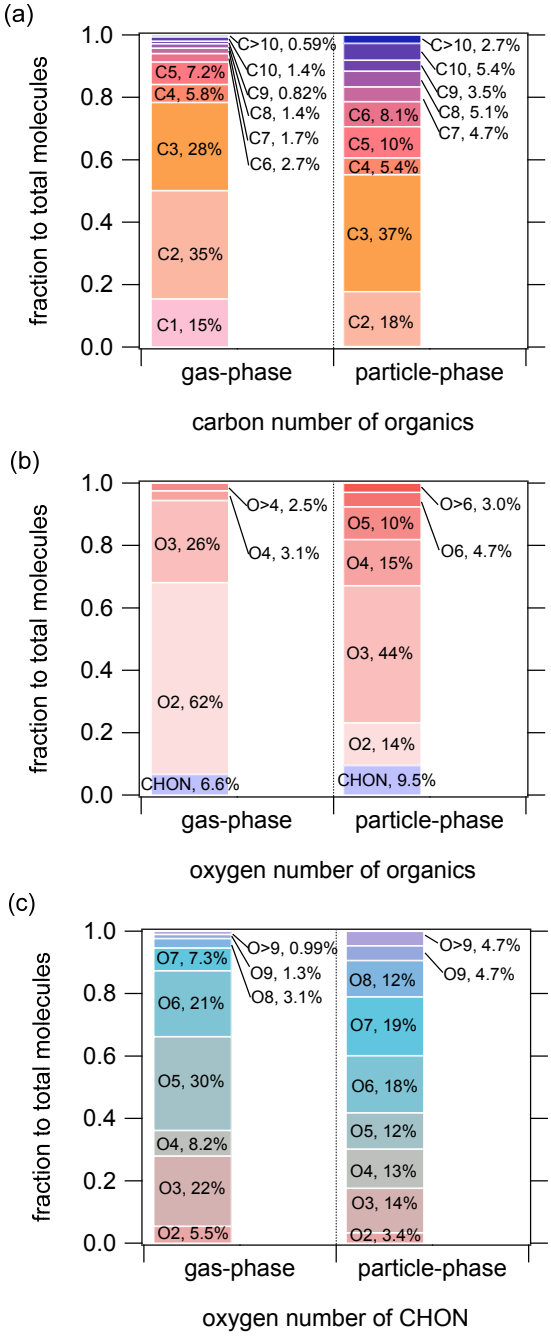

Figure 13. Carbon number distribution (a) and oxygen number distribution of total $C_xH_yO_z$ and $C_xH_yN_{1,2}O_z$ compounds (b), and oxygen number distribution of $C_xH_yN_{1,2}O_z$ compounds (c).

https://doi.org/10.5194/acp-2020-1187
Preprint. Discussion started: 25 November 2020

Atmospheric Chemistry and Physics Discussions

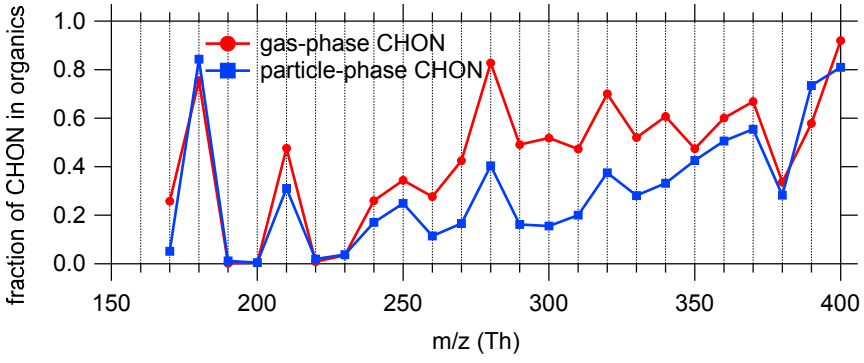

Figure 14. The average fractions of CHON to total organics (CHO + CHON + CHOS + CHONS) of every 10 Th in both phases. See Fig. S16 for the overall distribution of the contributions of species classes to the total concentrations.

https://doi.org/10.5194/acp-2020-1187
Preprint. Discussion started: 25 November 2020

Atmospheric Chemistry and Physics Discussions

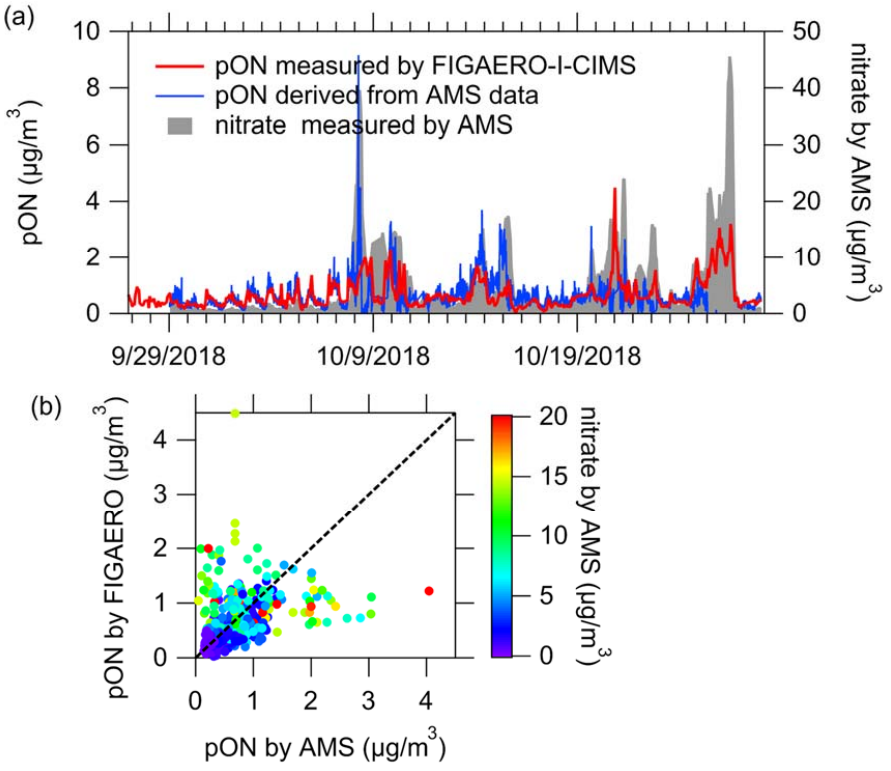

Figure 15. (a) Time series of particulate N-containing organics measured by FIGAERO-I-CIMS, particulate inorganic nitrate and organic nitrates derived from AMS data. (b) Comparison of particulate N-containing organics measured by FIGAERO-I-CIMS and particulate organic nitrates provided by AMS, color-coded by the concentrations of particulate inorganic nitrate measured by AMS.

https://doi.org/10.5194/acp-2020-1187
Preprint. Discussion started: 25 November 2020

Atmospheric Chemistry and Physics Discussions

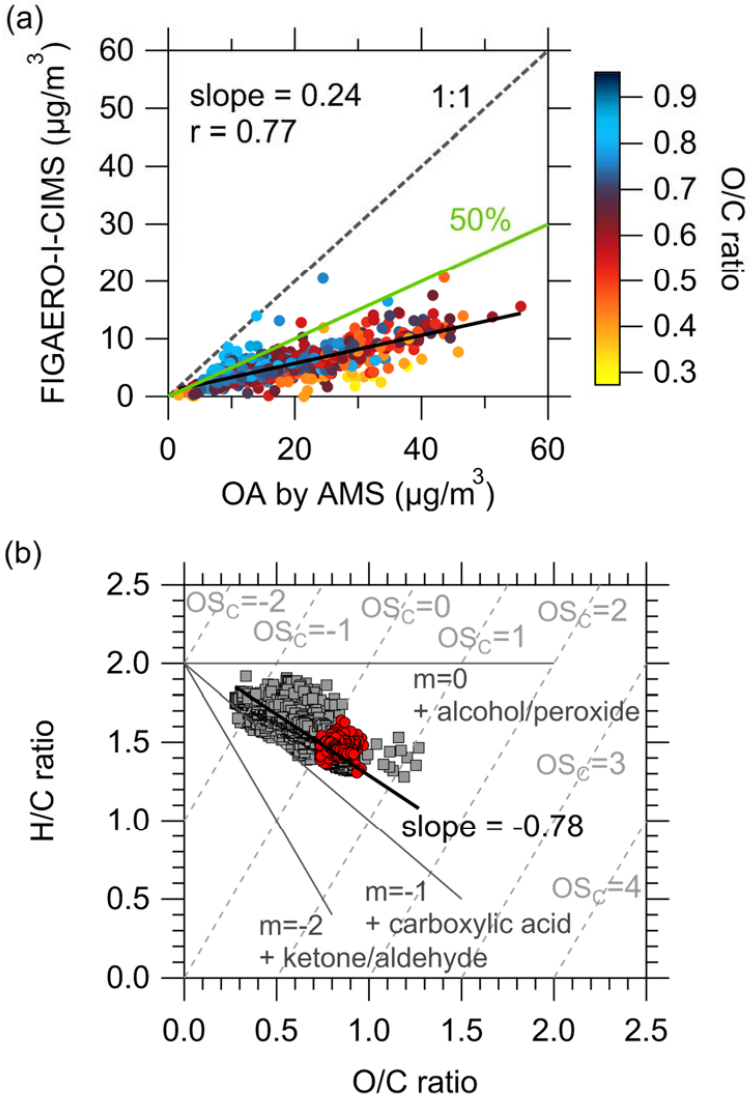

Figure 16. (a) Comparison of particulate organics measured by the FIGAERO-I-CIMS and AMS, color-coded by O/C ratios measured by AMS. The black line is the slope which represents the fraction of OA explained by the measurements of FIGAERO-I-CIMS. The green line shows the results from previous work which were ~50% (Lopez-Hilfiker et al., 2016; Stark et al., 2017). (b) Van Krevelen diagrams for organic aerosol derived from AMS data (gray squares) and FIGAERO-I-CIMS data (red circles). Black line is the slope of AMS data. Gray dotted lines are estimated carbon oxidation state.